Mediterranean Marine Science

HELLENIC CENTRE FOR MARINE RESEARCH

Mediterranean Marine Science

VOLUME 17 · Number 2 · (2016)

Concordant patterns of mtDNA and nuclear phylogeographic structure reveal Pleistocene vicariant event in the green crab Carcinus aestuarii across the Siculo-Tunisian Strait

T. DELI, N. CHATTI, K. SAID, C. D SCHUBART

To cite this article:

Research Article

Concordant patterns of mtDNA and nuclear phylogeographic structure reveal a Pleistocene vicariant event in the green crab *Carcinus aestuarii* across the Siculo-Tunisian Strait

T. DELI[1], N. CHATTI[1] , K. SAID[1] and C. D. SCHUBART[2]

[1] Laboratory of Genetics, Biodiversity and Enhancement of Bioresources (LR11ES41), University of Monastir,
Higher Institute of Biotechnology of Monastir, Av. Tahar Hadded, B.P. 74, Monastir 5000, Tunisia
[2] Faculty of Biology: Zoology and Evolution, University of Regensburg, D-93040 Regensburg, Germany

Corresponding author: temimdeli@yahoo.co.uk

Handling Editor: Fabio Crocetta

Abstract

This study focuses on the population genetic structure of the green crab *Carcinus aestuarii* along part of the African Mediterranean coast, with the main target being to confirm genetic subdivision across the well-documented genetic boundary of the Siculo-Tunisian Strait. For this purpose, the mitochondrial COI (cytochrome oxidase I) gene and five polymorphic microsatellite loci were analysed in 144 and 120 specimens, respectively. Our results show the existence of two distinct haplogroups separated by 16 mutational steps and revealed a non random distribution of the genetic variation along the African Mediterranean coast. Dating analyses, based on the use of different molecular clock models and rates, placed the divergence among both haplogroups at 1.91 Myr (95% HPD: 1.11–2.68 Myr) to 0.69 Myr (95% HPD: 0.44–0.98 Myr). This range of divergence time estimation corresponds to the Early Pleistocene. The particular pattern of genetic divergence among Eastern and Western African Mediterranean populations of *C. aestuarii*, detected by 2-level AMOVA at the mitochondrial level, was consistent with that inferred from microsatellite analysis and suggests a vicariant event in *C. aestuarii*. Demographic reconstruction, inferred from mismatch distribution and BSP analyses, yielded different patterns of demographic history between both African Mediterranean groups. The distribution pattern of the two haplogroups across the African Mediterranean coast, along with the results of a Bayesian analysis of genetic structure, revealed an intermediate geographic group between the two divergent groups of the African coast, thus supporting the hypothesis of secondary contact between two historically isolated groups. Although this hypothetical contact zone, thought to be located near the Siculo-Tunisian Strait, still needs to be verified, the asymmetric gene flow from the Western to the Eastern African Mediterranean, as inferred by the results of a MIGRATE analysis, reinforces the previously mentioned results.

Keywords: Brachyura, phylogeographic break, secondary contact, COI, microsatellites.

Introduction

Contemporary Mediterranean marine fauna bears a genetic legacy resulting from an extensive desiccation period between 5.59 and 5.3 million years ago, called the Messinian Salinity Crisis (Hsü *et al.,* 1977) that extirpated most species from the region or reduced species distributions to small isolated eastern refugia (Peres, 1985). Subsequent flooding of the Mediterranean Basin from the Atlantic was followed by episodic changes in sea levels associated with glacial cycles. Successive periods of colonization and isolation left longitudinal gradients in genetic diversity across the Mediterranean and in some cases resulted in great genetic diversity in the central Mediterranean as a result of bidirectional colonization and secondary contact (Arnaud-Haond *et al.,* 2007). Furthermore, the existence of a particularly complex oceanographic circulation pattern in the Mediterranean Sea (Astraldi *et al.,* 1999; Patarnello *et al.,* 2007), as well as several kinds of physical barriers such as straits and channels (Béranger *et al.,* 2004), play an important role

in shaping marine diversity and promoting genetic differentiation among populations of different species (e.g. Borsa *et al.,* 1997; Patarnello *et al.,* 2007).

The relatively narrow strait between north-eastern Tunisia and western Sicily, separating the Eastern and Western Mediterranean basins, constitutes one of the best documented biogeographical transition zones in the marine environment, shaped by both present and past physical oceanographic properties. During the last two million years, this region has been affected by dramatic geological events and climatic fluctuations, with the occurrence of numerous episodes of sea level regressions (Thiede, 1978) and notable diverse hydrographic features in both Mediterranean basins (Pinardi & Masetti, 2000). During the last glacial maximum (LGM, between 26,500-20,000 years before present; Clark *et al.,* 2009), oscillations of sea levels led to periods of reduced connectivity between the Eastern and Western basins, which stabilized about 11,000 years ago (Collina-Girard, 2001). Nowadays, the factors proposed to account for the maintenance of a biogeographical barrier in the area include the water cir-

culation pattern, characterized mainly by a constant and unidirectional east-south-east flow of a marine surface current arriving from Gibraltar (known as the Algerian Current) and bifurcating offshore of the north-eastern tip of the Tunisian coast. This contrasts with the rest of the Eastern Mediterranean Basin, which is characterized by very weak circulation (Pinardi & Masetti, 2000). Numerous studies have analysed variable mitochondrial or/and nuclear markers in populations of several vertebrate and invertebrate species around the Siculo-Tunisian Strait and suggested the existence of a genetic boundary in this region, which is probably the signature of past isolation events (e.g. Quesada *et al.*, 1995; Borsa *et al.*, 1997; Bahri-Sfar *et al.*, 2000; Nikula & Vainola, 2003; Zitari-Chatti *et al.*, 2009; Marino *et al.*, 2011; Ragionieri & Schubart, 2013; Deli *et al.*, 2015). The existence of similar divergence patterns among populations of different species from the Eastern and Western Mediterranean basins reinforce the idea that these Mediterranean species were facing the same historical oceanographic events. These resulted in vicariance across the Siculo-Tunisian Strait during Pleistocene glacial episodes, characterized by lower sea levels and surface temperatures in this region (Thiede, 1978).

The Mediterranean green crab *Carcinus aestuarii* (Nardo, 1847) has received much attention because of its success as a global invader and the longstanding debate regarding its classification (Bulnheim & Bahn, 1996; Geller *et al.*, 1997; Clark *et al.*, 2001; Behrens Yamada & Hauck, 2001; Roman & Palumbi, 2004). *C. aestuarii* is a very common inhabitant of estuaries and lagoons of the Mediterranean and Black seas (Mori *et al.*, 1990; Behrens Yamada & Hauck, 2001). It inhabits protected and often brackish habitats including subtidal and intertidal mud and sand in lagoons and estuaries, salt marshes and seagrasses (own observations). It is a voracious omnivore and aggressive competitor, and in parts of the Mediterranean subject to fisheries. It has a wide tolerance for salinity, temperature, oxygen, and thus habitat type (Mori *et al.*, 1990; Mistri *et al.*, 2001). Similarly to its closely related *Carcinus maenas*, *C. aestuarii* exhibits high fecundity and long planktonic larval stage of approximately six weeks (Darling *et al.*, 2008; Marino *et al.*, 2011). In the last few centuries, specimens of *C. aestuarii* have been accidentally introduced into several regions outside their native range as a result of maritime commerce and ballast transport: Canary Islands (Almaça, 1962), Tokyo Bay, Japan (Furota *et al.*, 1999) and South Africa (Geller *et al.*, 1997; Carlton & Cohen, 2003; Darling *et al.*, 2008).

With these life history characteristics, green crabs are expected to exhibit lack of population divergence and weakly or seemingly unstructured populations (Hilbish, 1996; Waples, 1998). Nevertheless, population genetic studies on *C. aestuarii* from native and invasive regions (Darling *et al.*, 2008; Marino *et al.*, 2010; 2011; Ragio-

nieri & Schubart, 2013) have revealed extensive genetic variability and population differentiation linked mainly to oceanographic discontinuities that characterize these areas. Specifically, Marino *et al.* (2011) and Ragionieri & Schubart (2013) found significant genetic differentiation among populations from the Western and Eastern European Mediterranean coastlines. Recently, a small-scale geographic survey of the genetic structure of *C. aestuarii*, based on restriction fragment length analyses of the mitochondrial cytochrome oxidase I (COI), revealed a sharp haplotypic discontinuity among Eastern and Western Mediterranean sites of Tunisia (Deli *et al.*, 2015). Both groups were found to be genetically and morphologically differentiated across the Siculo-Tunisian Strait (Deli *et al.*, 2014; 2015).

These interesting insights trigger the necessity of detailed phylogeographic and population genetic examinations of this species across the well-known biogeographic barrier of the Siculo-Tunisian Strait in order to describe and delimit divergent groups within this species in detail. These may reflect residual effects of vicariance events during Pleistocene glacial episodes, usually involved in generating genetic differentiation in marine invertebrates (Palumbi *et al.*, 1997). It would also allow confirming and detailing the phylogeographic break, as well as tracing back the evolutionary history of the green crab. To achieve these targets, samples from eleven African Mediterranean locations, covering parts of the Tunisian and Libyan coasts, and for comparison a population from Venice Lagoon, were collected and part of the COI gene was sequenced. In addition, we genotyped a set of polymorphic microsatellite loci specifically isolated and characterized for this species by Marino *et al.* (2008).

Material and Methods

Sampling and DNA extraction

Individuals of *C. aestuarii* were sampled during field missions from eleven locations along the African Mediterranean coast (Fig. 1). Crab legs from a population of the Venitian Lagoon (Italy) were included for population comparison and phylogeographical analysis. From each crab, muscle tissue was removed from a pereiopod and stored in absolute ethanol at -30 °C until needed. A total of 144 green crabs were used for mtDNA sequencing and 120 for microsatellite analysis (Table 1). Total genomic DNA was extracted from muscle tissue, using the Wizard® genomic DNA purification kit (Promega).

Mitochondrial DNA amplification and sequencing

A fragment of 658 basepairs (bp) of the mitochondrial COI was amplified using the primers COL6a and COH6, specifically designed for brachyuran crab species (see Schubart, 2009). The PCR reaction mix contained 13.5 µl ddH$_2$O, 2.4 µl dNTPs (1.25 mM), 2.5 µl 10x PCR

534

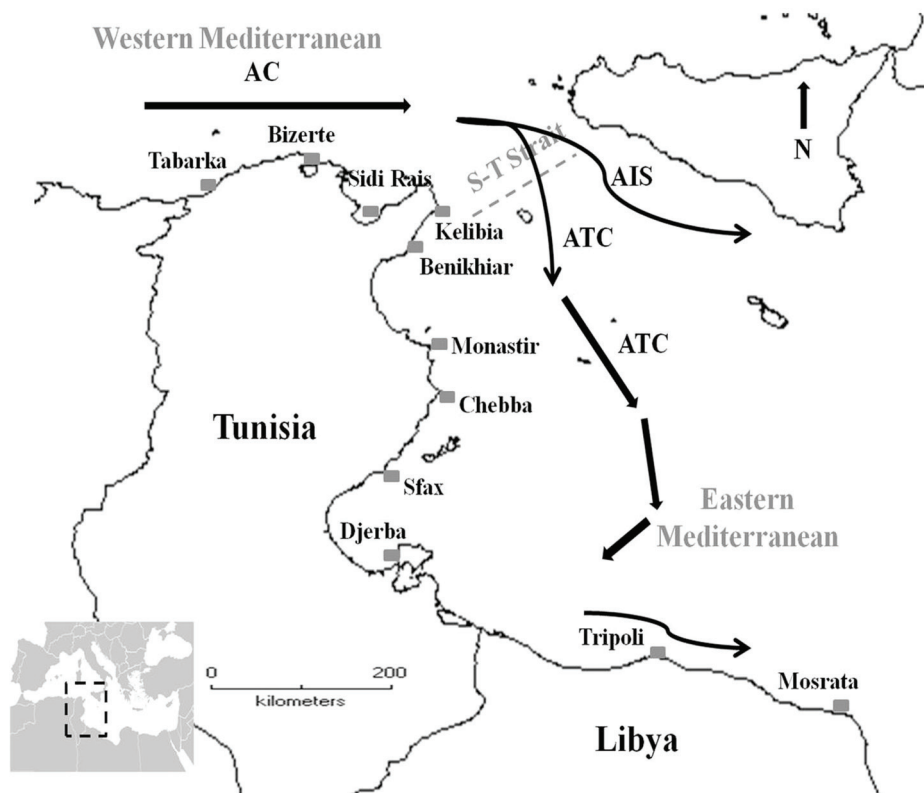*Medit. Mar. Sci., 17/2, 2016, 533-551*

Fig. 1: Sampling locations for the green crab *Carcinus aestuarii* along the African Mediterranean coast, and sea surface currents in the study region (according to Béranger *et al.,* 2004). (AC: Algerian Current; AIS: Atlantic Ionian Stream; ATC: Atlantic Tunisian Current).

buffer, 4 µl MgCl₂ (25mM), 0.3 µl of both primers, 1 µl Fermenters-TAQ (0.5 u) and 1 µl of diluted DNA, adding up to a final master mix volume of 25 µl. PCR amplifications were carried out with an initial denaturation phase of 4 min at 94°C, followed by 40 cycles, composed of 45 s of denaturation at 95°C, 60 s of annealing at 48°C and

Table 1. Sampling information on the green crab *Carcinus aestuarii* including collection sites, countries, regions, geographic coordinates and the number of specimens examined for mtDNA and microsatellite analyses.

Collection site	Country	Region	Geographic coordinates	Number of examined specimens	
				mtDNA	Microsatellite loci
Tabarka	Tunisia	Western Mediterranean	36°57′N 08°45′E	10	10
Bizerte	Tunisia	Western Mediterranean	37°16′N 09°52′E	15	10
Sidi Rais	Tunisia	Western Mediterranean	36°46′N 10°32′E	11	10
Kelibia	Tunisia	Western Mediterranean	36°51′N 11°05′E	10	10
Benikhia	Tunisia	Western Mediterranean	36°28′N 10°46′E	12	10
Monastir	Tunisia	Eastern Mediterranean	36°10′N 10°49′E	11	10
Chebba	Tunisia	Eastern Mediterranean	35°14′N 11°07′E	12	10
Sfax	Tunisia	Eastern Mediterranean	34°44′N 10°45′E	15	10
Djerba	Tunisia	Eastern Mediterranean	33°52′N 10°51′E	14	10
Tripoli	Libya	Eastern Mediterranean	32°54′N 13°11′E	11	10
Mosrata	Libya	Eastern Mediterranean	32°22′N 15°05′E	12	10
Venice Lagoon	Italy	Eastern Mediterranean	45°27′N 12°16′E	11	10

completed with an extension of 60 s at 72°C. These cycles were followed by 8 min of final extension at 72°C. PCR products were loaded and visualized on 1.5 % agarose gel. Strong products were outsourced for sequencing with primer COL6a to LGC Genomics (Berlin). The obtained sequences were visually corrected with Chromas Lite, aligned with Clustal W, implemented in BIOEDIT (Hall, 1999), and trimmed to a 613 bp fragment for subsequent analyses.

Medit. Mar. Sci., 17/2, 2016, 533-551

535

Microsatellite loci amplification and allele sizing

A total of 120 individuals of *C. aestuarii* were screened for polymorphisms at five variable microsatellite loci (Cae01, Cae07, Cae33, Cae71 and Cae86), specifically isolated and described for the green crab (Marino *et al.,* 2008). DNA amplification was carried out in 10.2 μl reactions under the following conditions: 6 μl ddH$_2$O, 1 μl dNTPs (1.25 mM), 1 μl 10x PCR buffer, 0.5 μl MgCl$_2$ (25mM), 0.2 μl of both primers, 1 μl Fermenters-TAQ (0.5 u) and 1 μl of diluted DNA. PCR thermal cycling conditions include 35 cycles with 30 s for denaturation at 94°C, 30 s for annealing at 50°C-56°C (annealing temperatures specific to the studied loci as indicated in Marino *et al.,* 2008) and 30 s for extension at 72°C, preceded by 4 min of initial denaturation at 94°C and followed by 10 min of final extension at 72°C. For the detection of polymorphisms, the forward primer for each locus was 5'-labelled, and labelled amplicons from the five loci were combined into three different sets (Cae01 FAM + Cae07 VIC; Cae33 NED + Cae71 FAM; and Cae86 VIC). For each set, 1 μl of each diluted PCR product was loaded with 25 μl of formamide and 0.5 μl of size standard TAMRA 500 in a final volume of 26.5 μl for successive dimensional analysis. Sizing was performed in an ABI Prism 310 Genetic Analyzer (Applied Biosystems) of the University of Regensburg with reference to the internal size standard TAMRA 500 using Genotyper ver. 3.5 and GeneScan ver. 3.5 (Applied Biosystems).

Statistical analysis of mtDNA data

The nucleotide composition was assessed with MEGA, version 5.2 (Tamura *et al.,* 2011). Measurements of DNA polymorphism, including number of haplotypes (*N*h), number of polymorphic sites (*N*ps), haplotype diversity (*h*; Nei, 1987), nucleotide diversity (π; Tajima, 1983; Nei, 1987), and mean number of nucleotide differences (K) were calculated for each population using DNASP, version 5.10 (Librado & Rozas, 2009).

A statistical parsimony network, implemented in TCS software, version 1.21 (Clement *et al.,* 2000), was constructed in order to infer intraspecific evolutionary relationships among the COI haplotypes of *C. aestuarii*. This method uses coalescence theory (Hudson, 1990) to determine the limits of parsimony and define a set of plausible connections among haplotypes that have accumulative probability of more than 95 % of being true (Templeton *et al.,* 1992). The distribution pattern of the corresponding haplotypes was examined across the African Mediterranean coast. COI haplotypes were used to compute both levels of population subdivision using unordered (G_{ST}) and ordered haplotypes (N_{ST}) in order to assess the relationship between phylogeny and the geographical distribution of haplotypes, and test the presence of phylogeographic structure. These parameters were estimated following the methods described by Pons & Petit (1995; 1996) using PERMUT & CPSRR, version 2.0 (Pons & Petit, 1996). G_{ST} is solely based on haplotype frequencies, whereas N_{ST} also takes into account the genetic relationship among haplotypes. A N_{ST} higher than the G_{ST} usually indicates the presence of phylogeographic structure (Pons & Petit, 1996; Petit *et al.,* 2005), i.e. if closely-related haplotypes are more often found in the same area than less closely-related haplotypes. Finally, these two parameters were compared using the *U*-test (Pons & Petit, 1996).

Divergence time between the resulting mitochondrial haplogroups was estimated using BEAST, version 1.7.5 (Drummond *et al.,* 2012), considering the closure of the Gibraltar Strait at the start of the Messinian Salinity Crisis (5.59 million years ago; Krijgsman *et al.,* 1999) as calibration point for rate estimation. During the Messinian Salinity Crisis, the contact between the Mediterranean and the Atlantic Ocean was interrupted, thus providing the geographic barrier necessary for the speciation of *C. aestuarii* and *C. maenas* (Demeusy, 1958; Geller *et al.,* 1997). A simplified phylogenetic approach was used, ignoring the intraspecific nature of our data. The Birth-Death process (Rannala & Yang, 1996; Yang & Rannala, 1997), including only unique haplotype sequences, corresponding to the encountered *C. aestuarii* haplogroups and the Atlantic sister species *C. maenas* respectively, were used as a tree prior model of speciation. Analyses were carried out with an uncorrelated lognormal relaxed clock (Drummond *et al.,* 2006). The normal distribution with a standard deviation of 55,000 years (Marino *et al.,* 2011) was used to incorporate the calibration priors on the root of the tree. The use of deep calibration points derived from biogeographic events could bias recent divergence times, resulting in divergence estimates older than their actual age (Burridge *et al.,* 2008). In order to avoid such uncertainty and obtain a comprehensive estimation of divergence time among obtained green crab haplogroups, additional analyses involving the entire intra-specific data of *C. aestuarii* were performed using a strict molecular clock and assuming the GTR model of sequence evolution, as calculated by MODELTEST, version 3.7 (Posada & Crandall, 1998), and a coalescent tree prior. Two different clock rates for the COI gene were tested in order to obtain a comprehensive view on divergence estimation: 1.4 % per million years (Myr) as calculated for this gene in the Panamanian snapping shrimp *Alpheus* (see Knowlton & Weight, 1998) and a specifically estimated mutation rate for *Carcinus* of 3.86 % per Myr (see Marino *et al.,* 2011). For all kinds of analyses, the Markov chain Monte Carlo (MCMC) simulations were run for 100 million steps and sampled every 1000 steps. All Bayesian outputs, produced through BEAST, were also reviewed in TRACER, version 1.5 (Rambaut & Drummond, 2007) for robustness in a similar manner to the MrBayes simulations. We summarized the resultant trees in TreeAnnotator to create a 50 % majority

536

Medit. Mar. Sci., 17/2, 2016, 533-551

rule consensus maximum clade credibility tree. FigTree, version 1.4.0 (Rambaut, 2009), was used to exhibit the results.

Evidence of population genetic differentiation was assessed by 1-level AMOVA (Analysis of molecular variance) (Excoffier et al., 1992), as implemented in ARLEQUIN, version 3.1 (Excoffier et al., 2005), based on nucleotide diversity and haplotype frequency. The extent of genetic differentiation between populations was estimated using the fixation indices: Φ_{ST} (based on the Tajima-Nei model, suggested for unequal nucleotide frequencies, as observed in our dataset; Tajima & Nei, 1984) and F_{ST} (computed using haplotypic frequency). Significance levels of pairwise genetic distances, estimated among populations, were assessed by a randomization procedure with 10,000 permutations. Test of isolation by distance was assessed by the Mantel Test, as implemented in the AIS (Alleles in Space) program, version 1.0 (Miller, 2005). The statistical significance of the test was assessed by running 10,000 random permutations. Analysis of molecular variance (2-level AMOVA) was also used to examine population genetic structure of C. aestuarii under two biogeographic hypotheses: (1) Western Mediterranean vs. Eastern Mediterranean basins and (2) Western African Mediterranean vs. Eastern African Mediterranean vs. Adriatic Sea. Additional AMOVA analyses were carried out, considering only African Mediterranean populations and aimed at testing genetic subdivision within the investigated region (Western African Mediterranean vs. Eastern African Mediterranean). In order to obtain a comprehensive view on the population genetic structure of C. aestuarii, we also investigated the relationship between genetic distance and geographic location of the twelve studied populations of the green crab, using the spatial analysis of molecular variance (SAMOVA) approach implemented in SAMOVA, version 1.0 (Dupanloup et al., 2002). This method allows defining groups of geographically proximate populations that are maximally differentiated from each other, through a simulated annealing procedure without prior assumption of group composition. The program was run with 100 random initial conditions for 10,000 iterations, testing for the grouping options from a predefined number of groups (K = 2-7).

Signatures of population demographic changes were investigated in African Mediterranean C. aestuarii populations using three neutrality tests: Tajima's D (Tajima, 1989), Fu's Fs (Fu, 1997), and Ramos-Onsins & Rozas's R_2 (Ramos-Onsins & Rozas, 2002), in addition to mismatch distribution (MMD) and Bayesian Skyline Plots (BSP) analyses. Based on the outcome of population genetic structure, MMD and BSP demographic analyses were performed separately for the two differentiated groups of the Western and Eastern African Mediterranean (as identified by AMOVA analyses).

The examination of deviation from neutrality by both D and Fs indices was based on 1000 coalescent simulations, as implemented in ARLEQUIN. R_2 statistics of Ramos-Onsins & Rozas (2002) was calculated using a coalescent simulation algorithm implemented in DNASP with 1000 simulations. Demographic changes in C. aestuarii were also examined by calculating Harpending's raggedness index rg (Harpending, 1994) of the observed mismatch distribution for each of the populations according to the population expansion model implemented in ARLEQUIN, and its significance was tested using parametric bootstrapping (10,000 replicates). These indices were calculated for each population and the whole dataset.

To provide other estimates of population size changes, we also examined site mismatch distributions for the Western and Eastern African Mediterranean basins. Contrasting plots of observed and theoretical distributions of site differences provide insight into past population demographics. The expected mismatch distributions under a sudden expansion model were computed in ARLEQUIN. The sum of squared deviations (SSD) between observed and expected distributions was used as a measure of fit, and the probability of obtaining a simulated SSD greater than or equal to the expected was computed by randomization. If this probability was > 0.05, the expansion model was accepted. Graphical representation was carried out by means of the growth-decline model implemented in DNASP. Range expansion in C. aestuarii groups was investigated by the spatial expansion model, as implemented in ARLEQUIN (Excoffier, 2004).

The magnitude of historical demographic events for the African Mediterranean regions of C. aestuarii was investigated using Bayesian Skyline Plots (BSP, Drummond et al., 2005). In comparison with simple parametric and older coalescent demographic methods, the smoother estimates and sensitivity of this method, together with a credibility interval, provide a realistic population size function and enable retrieval of more details than just summary statistics. Furthermore, estimation of time since expansion event is much more accurate with BSP than with the expansion parameter Tau (τ), inferred from the mismatch distribution analysis, as recent expansions in a BSP are not affected by deep coalescences (Grant, 2015). Analyses were run in BEAST, version 1.7.5, using a GTR model and a strict molecular clock, implementing the specific mutation rate of 3.86 % per Myr, estimated for Carcinus by Marino et al. (2011). The Markov chain Monte Carlo simulations were run with 30,000,000 iterations, while genealogies and model parameters were sampled every 1000 iterations. Two independent runs were carried out. The first 3,000,000 iterations were discarded as burn-in, whereas the remaining results were combined in LogCombiner and summarized as BSPs after analysing their convergence (Effective Sample Sizes (ESS) of all parameters > 200 for each group) in TRACER, version 1.5.

Medit. Mar. Sci., 17/2, 2016, 533-551

537

Statistical analysis of microsatellite data

The dataset was checked for genotyping errors (i.e. null alleles) by means of equation 2 from Brookfield (1996), as implemented in MICRO-CHECKER, version 2.2.3 (Van Oosterhout *et al.,* 2004). Deviations from Hardy-Weinberg equilibrium (HWE) in the Mediterranean green crab populations were tested using the Markov chain method with 5000 iterations as implemented in GENEPOP, version 4.2 (Raymond & Rousset, 1995). Genetic variability at the typed microsatellite loci (Ar: allelic richness, Ho: observed heterozygosity and He: expected heterozygosity) as well as Weir & Cockerham (1984) estimation of F_{IT}, F_{ST} and F_{IS} were calculated using FSTAT, version 9.2.3.2 (Goudet, 1995). Genetic diversity measures for each population (Ho: observed heterozygosity, He: expexted heterozygosity and F_{IS}: inbreeding coefficient) were estimated with GENEPOP using the Markov chain parameter with 10,000 dememorizations, 20 batches, and 5000 iterations per batch.

Genetic differentiation was estimated by means of the exact test (G) of population differentiation (Raymond & Rousset, 1995), as implemented in GENEPOP. This test verifies the existence of differences in allele frequencies at each locus and for each population. Single locus *P* values were calculated using a Markov chain with 10,000 dememorizations, 100 batches, and 5000 iterations per batch, combined over loci using the Fisher exact test. The existence of genetic differentiation was also assessed by 1-level AMOVA (Excoffier *et al.,* 1992), using ARLEQUIN, version 3.1. Pairwise comparisons of genetic differentiation were estimated from the χ2 of the Fisher exact test and the F_{ST} values. Level of significance (*P*) was computed by permutation tests from 10,000 random permutations for F_{ST} values and estimated by the Markov chain algorithm (10,000 dememorizations, 100 batches, and 5000 iterations per batch) for χ^2 values. Correlations between genetic (F_{ST} values) and geographic distances were assessed by the Mantel Test, as implemented in ARLEQUIN, with 10,000 random permutations. Additional 2-level AMOVA was performed grouping populations according to the tested biogeographic hypotheses with mtDNA data.

The Bayesian approaches implemented in the software packages STRUCTURE, version 2.3.4 (Pritchard *et al.,* 2000), and BAPS, version 3.2 (Corander *et al.,* 2003), were also used to identify clusters of genetically similar populations based on the nuclear microsatellite data. BAPS generally tends to recover more clusters than STRUCTURE, and it has been suggested that both approaches should be used, particularly where levels of differentiation between populations might be low (Latch *et al.,* 2006). For STRUCTURE analysis, the model without admixture was processed using correlated allele frequencies. The models without admixture assume that the sample is a mixture of *K* diverging subpopulations. Individuals were then probabilistically assigned to the *K* genetic clusters (Francois &

Durand, 2010). The probability of the number of populations (*K*) was estimated by fixing prior values of *K* (from 1 to 12 in our study) and comparing the *Ln* P (D) (the log probability of the data) and the log likelihood of the data. Three replicates for each K were independently performed, providing reproducible results. The most likely number of independent population clusters was verified using the ΔK method of Evanno *et al.* (2005). The analysis was run for 500,000 generations with a burn-in of 20,000 iterations. For BAPS analysis, the number of genetically diverged groups (*K*) in both clustering of individuals and clustering of groups of individuals corresponded to the highest log marginal likelihood of the data (log (ml)). Burn-in period of 10,000 iterations was used followed by 50,000 iterations.

Genotypic assignment was also assessed by GENE-CLASS, version 2.0 (Piry *et al.,* 2004). The most probable origin of each individual was calculated by comparing the likelihood of the multi-locus genotype of a given individual in a set of pre-determined populations. The Bayesian method, proposed by Rannala & Mountain (1997), was chosen together with a threshold of 0.05. GENECLASS also allowed detecting the number of migrants. The frequencies-based method described by Paetkau *et al.* (1995) was used and a threshold of 0.01 was set. For both tests, the rejection probability was obtained by simulating 10,000 individuals from allelic frequencies based on the simulation algorithm of Paetkau *et al.* (2004).

Contemporary gene flow analysis and migration patterns among Western and Eastern African Mediterranean groups of populations of *C. aestuarii* (group 1: Tabarka, Bizerte, Sidi Rais, Kelibia, Benikhiar; group 2: Monastir, Chebba, Sfax, Djerba, Tripoli, Mosrata) were evaluated using MIGRATE-n, version 3.6, software (Beerli, 2006). MIGRATE estimates migration rates *M* and effective population sizes *Θ* among both regional groups, based on the analysis of the examined loci. A Brownian mutation model was used and the mutation considered was constant for all loci. MIGRATE software uses a maximum-likelihood (ML) framework based on the coalescence theory and investigates possible genealogies with migration events using a Markov chain Monte Carlo approach (Beerli & Felsenstein, 2001). For each locus, the ML was run for chains with 5000 and 50,000 recorded genealogies, respectively, after discarding the first 10,000 genealogies (burn-in). Unlike estimates of gene flow using *F*-statistics, MIGRATE-n allows asymmetrical migration rates among both investigated groups of populations (*M*1→2 and *M*2→1) separated by barriers to gene flow as identified by AMOVA, STRUCTURE and BAPS. Thus, these estimates were used to report the estimated main direction of gene flow across the recognised biogeographic barrier (Siculo-Tunisian Strait).

538

Medit. Mar. Sci., 17/2, 2016, 533-551

Results

Mitochondrial DNA

Sequences corresponding to the mtDNA COI gene from 144 individuals and twelve locations of *C. aestuarii* were proofread and trimmed to an alignment length of 613 bp. A total of 60 nucleotide sites were variable, of which 42 were parsimony-informative. Among these sequences, 54 haplotypes were identified. The nucleotide composition of the analyzed fragment showed an A-T bias (C = 18.53 %; T = 36.15 %; A = 26.35 %; G = 18.97 %), which is typical of invertebrate mitochondrial DNA (Simon *et al.,* 1994).

Overall, genetic diversity analyses of this mitochondrial dataset showed high haplotype ($h = 0.888 \pm 0.021$) and nucleotide ($\pi = 0.0122 \pm 0.001$) diversities (Table 2). The mean number of nucleotide differences (K) can also be considered as high (K = 7.5) and ranged from 0.166 in the population of Benikhiar to 12.164 in Djerba (Table 2). A remarkable difference in this parameter was shown mainly among the northwest African populations (Tabarka, Bizerte, Sidi Rais, Kelibia, Benikhiar) and their north-eastern counterparts (Monastir, Chebba, Sfax, Djerba, Tripoli, Mosrata). The latter group of populations exhibited higher levels in the mean number of nucleotide differences (Table 2) suggesting possible genetic subdivision within the analyzed data. The statistical parsimony procedure revealed the existence of two haplogroups, each characterized by a star-like shape and separated by 16 mutational steps (Fig. 2). These two haplogroups were centered on two main haplotypes, 2 and 29 respectively, distinguished by 19 mutational steps. A clear separation was also noted within the second haplogroup, in which haplotype 29 was distinguished from haplotype 40 by 12 mutational steps. The latter haplotype was found in two specimens from the populations of Djerba and Mosrata (Fig. 2). The first haplogroup (type I) was represented in all populations while the second (type II) was mainly found in the Eastern African Mediterranean populations of Tunisia (Monastir, Chebba, Sfax, Djerba) and Libya (Tripoli, Mosrata). Calculations of N_{ST} (0.179) and G_{ST} (0.081) revealed that the N_{ST} value was significantly higher than the G_{ST} value ($P < 0.01$), inferring a significant relationship between phylogeny and the geographical distribution of haplotypes, and indicating the existence of phylogeographic structure among the examined samples.

The distribution pattern of the two haplogroups across the African Mediterranean coast showed that the proportion of type I, dominant in Western Mediterranean populations, decreases notably in the Eastern counterparts (Fig. 3). Both types, I and II, were shown to be mixed in the Eastern Mediterranean. Divergence time between the two mitochondrial types was estimated based on different models and calibration strategies. In a first analysis, including only unique haplotypes, using a 5.59 Myr split between *C. aestuarii* and *C. maenas* as calibration point (Krijgsman *et al.,* 1999) and assuming a Birth-Death prior and uncorrelated lognormal relaxed clock, Bayesian phylogenetic analysis estimated divergence among both haplogroups to occur approximately around 1.20 Myr (95%

Table 2. Mitochondrial and nuclear diversity measures for each population of *Carcinus aestuarii* as well as for the entire sample. *N*: sample size for each population; *N*h: number of haplotypes; *N*ps: number of polymorphic sites; *h*: haplotype diversity; K: mean number of nucleotide differences; π: nucleotide diversity; *P*: the *P*-value of departure from the Hardy-Weinberg equilibrium (values in bold indicate significant departure from H-W equilibrium); *H*o: observed heterozygosity; *H*e: expected heterozygosity; F_{IS}: inbreeding coefficient.

Genetic marker			Mitochondrial COI gene			Microsatellite loci				
Population	N	Nh	Nps	h	K	π	N	P	Ho	He	F_{IS}
Tabarka	10	5	6	0.755 ± 0.130	1.355	0.0022 ± 0.000	10	0.625	0.880	0.875	-0.005
Bizerte	15	8	10	0.866 ± 0.067	1.771	0.0028 ± 0.000	10	0.076	0.860	0.914	0.059
Sidi Rais	11	5	23	0.709 ± 0.137	4.600	0.0075 ± 0.004	10	0.118	0.840	0.896	0.063
Kelibia	10	5	6	0.666 ± 0.163	1.355	0.0022 ± 0.000	10	0.137	0.880	0.915	0.038
Benikhiar	12	2	1	0.166 ± 0.134	0.166	0.0002 ± 0.000	10	0.445	0.920	0.926	0.007
Monastir	11	9	30	0.945 ± 0.066	8.781	0.0143 ± 0.005	10	0.205	0.920	0.912	-0.008
Chebba	12	11	33	0.984 ± 0.040	10.242	0.0167 ± 0.004	10	0.058	0.840	0.901	0.067
Sfax	15	13	30	0.971 ± 0.039	10.838	0.0176 ± 0.002	10	**0.007**	0.800	0.902	0.113
Djerba	14	9	32	0.912 ± 0.059	12.164	0.0198 ± 0.002	10	0.192	0.880	0.896	0.018
Tripoli	11	7	25	0.909 ± 0.066	5.781	0.0094 ± 0.004	10	0.415	0.920	0.928	0.009
Mosrata	12	9	31	0.939 ± 0.058	9.893	0.0161 ± 0.004	10	**0.000**	0.780	0.900	0.133
Venice Lagoon	11	8	11	0.945 ± 0.054	3.745	0.0061 ± 0.000	10	0.068	0.820	0.916	0.105
Total	144	54	60	0.888 ± 0.021	7.500	0.0122 ± 0.001	120	0.195	0.861 ± 0.038	0.907 ± 0.011	0.050 ± 0.040

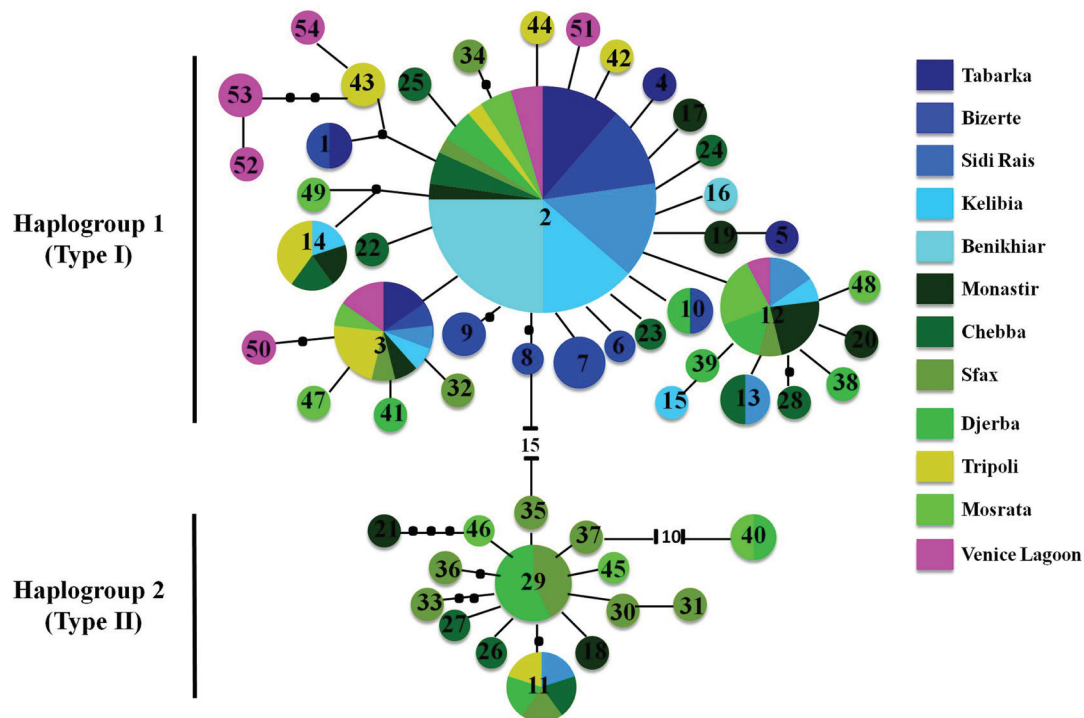*Medit. Mar. Sci.,* 17/2, 2016, 533-551

539

Fig. 2: TCS haplotype network of *Carcinus aestuarii*, based on the alignment of 613 bp of the mitochondrial gene COI, showing the relationships among the recorded haplotypes. Haplotype 2 corresponds to the ancestral haplotype. Each line between two points represents one mutational step. Circle size depicts proportions of haplotypes; the smallest corresponds to 1 and the largest to 44 individuals.
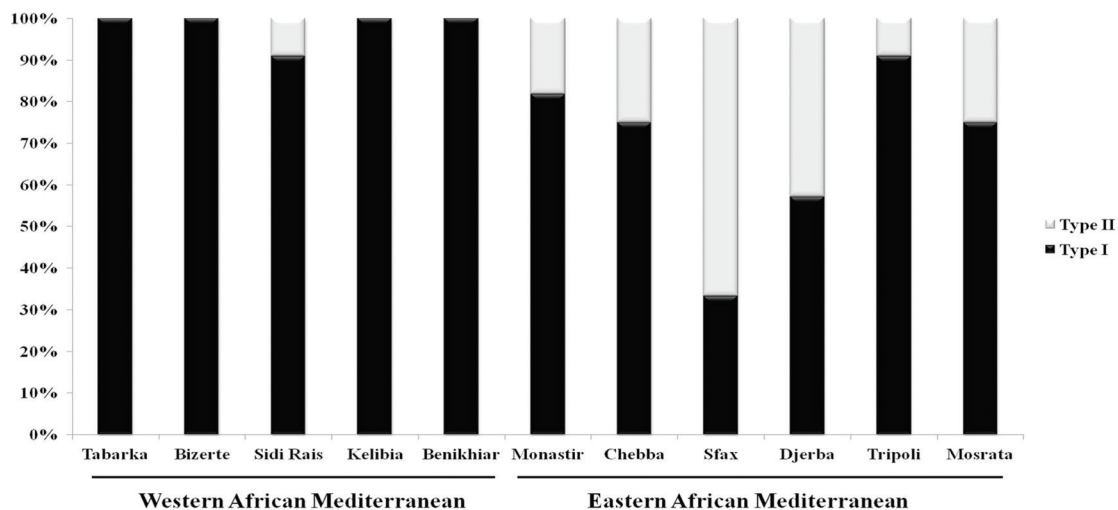

Fig. 3: The distribution pattern of the two types of haplogroups in *Carcinus aestuarii* along the African Mediterranean coast.

HPD (high posterior density interval): 0.51-1.68 Myr). Using a strict molecular clock, and assuming the GTR model of sequence evolution and a coalescent tree prior, involving the entire intra-specific data of *C. aestuarii*, the time to the most recent common ancestor (tMRCA) was estimated

at 1.91 Myr (95% HPD: 1.11–2.68 Myr), when applying the substitution rate of 1.4 % per million years (Myr) (see Knowlton & Weight, 1998). Estimated time of the split between the two haplogroups was notably younger (0.69 Myr (95% HPD: 0.44–0.98 Myr)), based on the species-

specific mutation rate of 3.86 % per Myr calculated and used by Marino *et al.* (2011) for *Carcinus*.

The 1-level AMOVA evidences highly significant genetic differentiation among examined populations of *C. aestuarii*, based on Tajima-Nei distances and haplotype frequencies (Table 3). The Mantel Test revealed non-significant correlation between genetic and geographic distances (r = -0.072, P = 0.739), suggesting absence of obvious isolation due to distance. Pairwise comparisons of genetic differentiation, estimated from genetic divergence and haplotype frequencies, showed that the majority of significant values were those between the Eastern and Western Mediterranean populations (Table 4). Based on these insights, we carried out a 2-level AMOVA in order to test the genetic structure of the *C. aestuarii* population under the two possible biogeographic hypotheses: (1) Western Mediterranean vs. Eastern Mediterranean and (2) Western African Mediterranean vs. Eastern African Mediterranean vs. Adriatic Sea. Overall, genetic structure was significant under both biogeographic scenarios, with the first hypothesis explaining better the genetic separation among samples (Table 3). Considering only African Mediterranean populations for AMOVA analyses, genetic differentiation among populations was highly significant (1-level AMOVA: Φ_{ST} = 0.190, P < 0.001, based on Tajima-Nei distances; F_{ST} = 0.087, P < 0.001, based on haplotype frequencies) and genetic structure, testing the separation between Western and Eastern African Mediterranean groups, was much more pronounced (2-level AMOVA:

Φ_{CT} = 0.192, P < 0.01, based on Tajima-Nei distances; F_{CT} = 0.105, P < 0.01, based on haplotype frequencies; Table 3). Spatial analysis of molecular variance (SAMOVA), depicting patterns of population structure within the examined dataset, showed that partitioning of variance among groups (Φ_{CT}) was highest in the case of three hierarchical groups (K = 3: [Sfax] vs. [Djerba] vs. [Tabarka + Bizerte + Sidi Rais + Kelibia + Benikhiar + Monastir + Chebba + Tripoli + Mosrata + Venice]; Φ_{CT} = 0.365, P = 0.011). Spatial distribution of genetic structure revealed the existence of genetic separation between the south-eastern Mediterranean populations of Sfax and Djerba and the remaining populations. The results also agree with the phylogeographic signal inferred from the COI haplotype network and confirm the general trend of genetic separation between the Eastern and Western Mediterranean basins, as inferred from the AMOVA results.

Population demographic history was reconstructed using three neutrality tests, mismatch distribution, and BSP analyses. The applied neutrality tests (D, F_S, and R_2 tests) revealed significant deviations from mutation-drift equilibrium for the populations of Bizerte, Sidi Rais, Kelibia and Benikhiar (Table 5) and suggest recent events of population expansion. For the whole dataset, departure from neutrality was inferred from Fu's F_S (-24,537, P < 0.001).

At the regional scale, focusing mainly on the Western and Eastern African Mediterranean, mismatch distribution analysis showed unimodal variation for the western populations (Fig. 4a), which is consistent with a recent

Table 3. Analysis of molecular variance testing for genetic differentiation among studied populations of *Carcinus aestuarii* and partition of the genetic variance under different biogeographic hypotheses. Significant values are in bold, calculated from 10,000 permutations.

Partition tested	mtDNA		Microsatellite loci Distance method: Number of different alleles (F_{ST})
	Nucleotide divergence (Tajima and Nei distance)	Haplotype frequency	
Considering all examined populations			
Among locations: Tabarka, Bizerte, Sidi Rais, Kelibia, Benikhiar, Monastir, Chebba, Sfax, Djerba, Tripoli, Mosrata, Venice Lagoon.	Φ_{ST} = **0.193** (P < 0.001)	F_{ST} = **0.080** (P < 0.001)	F_{ST} = **0.018** (P < 0.001)
Among: Western Mediterranean (Tabarka, Bizerte, Sidi Rais, Kelibia, Benikhiar) vs. **Eastern Mediterranean** (Monastir, Chebba, Sfax, Djerba, Tripoli, Mosrata, Venice Lagoon).	Φ_{SC} = **0.117** (P < 0.01) Φ_{ST} = **0.251** (P < 0.001) Φ_{CT} = **0.151** (P < 0.05)	F_{SC} = **0.026** (P < 0.05) F_{ST} = **0.124** (P < 0.001) F_{CT} = **0.100** (P < 0.001)	F_{SC} = **0.016** (P < 0.001) F_{ST} = **0.021** (P < 0.001) F_{CT} = **0.005** (P < 0.05)
Among: Western African Mediterranean (Tabarka, Bizerte, Sidi Rais, Kelibia, Benikhiar) **vs. Eastern African Mediterranean** (Monastir, Chebba, Sfax, Djerba, Tripoli, Mosrata) **vs. Adriatic Sea** (Venice Lagoon).	Φ_{SC} = **0.091** (P < 0.05) Φ_{ST} = **0.246** (P < 0.001) Φ_{CT} = 0.171 (P = 0.084)	F_{SC} = **0.027** (P < 0.05) F_{ST} = **0.111** (P < 0.001) F_{CT} = **0.086** (P < 0.01)	F_{SC} = **0.013** (P < 0.001) F_{ST} = **0.021** (P < 0.001) F_{CT} = **0.008** (P < 0.01)
Considering African Mediterranean populations			
Among: Western African Mediterranean (Tabarka, Bizerte, Sidi Rais, Kelibia and Benikhiar) **vs. Eastern African Mediterranean** (Monastir, Chebba, Sfax, Djerba, Tripoli and Mosrata).	Φ_{SC} = **0.086** (P < 0.05) Φ_{ST} = **0.262** (P < 0.001) Φ_{CT} = **0.192** (P < 0.01)	F_{SC} = **0.028** (P < 0.05) F_{ST} = **0.131** (P < 0.001) F_{CT} = **0.105** (P < 0.01)	F_{SC} = **0.026** (P < 0.05) F_{ST} = **0.124** (P < 0.001) F_{CT} = **0.100** (P < 0.001)

Medit. Mar. Sci., 17/2, 2016, 533-551

541

demographic expansion event. Nevertheless, multimodal distribution was clearly revealed for the Eastern African Mediterranean group (Fig. 4c). Statistical analysis of mismatch distributions, yielding non-significant values for the two demographic indices SSD and rg, allowed accepting the model of demographic expansion for both groups (Fig. 4a, c). A spatial expansion model was only accepted for the Western African Mediterranean (SSD = 0.000; P = 0.873, associated with a strictly positive migration rate: M = 7.852 [1.049-99999, for a 95 % confidence interval]).

Demographic history of the two African Mediterranean regions of $C.$ $aestuarii$ was also inferred from the coalescent approach of the BSP analysis. The pattern of effective population size evolution over time showed a sudden and recent increase in the effective size of the population, following a short phase of decrease in numbers. These two phases were preceded by quite a long stationary period (Fig. 4b, d). Overall, the BSP results were well concordant with those inferred from mismatch distribution and revealed that the expansion time occurred approximately about 33,300 years ago (CI: 18,750-43,750 years ago) for the Western African Mediterranean and about 29,166 years ago (CI: 25,000-50,000 years ago) for the Eastern African Mediterranean. Notably, the increase in effective size was much more pronounced in the Eastern African group (Fig. 4d). Expansion events for both regions were seemingly preceded by recent declines or bottleneck events, even if the retrieved signals might not be significant, as clearly shown by the fact that the slight lowering of the median traces is well included in the wide highest 95 % posterior density intervals of the demographic functions (Fig. 4b, d).

Microsatellite loci

Overall, a total of 152 alleles were detected at the five genotyped microsatellite loci. MICRO-CHECKER analysis of the dataset revealed absence of null alleles for the examined loci. All loci were polymorphic, with the number of alleles per locus ranging from 11 (locus Cae01) to 42 (locus Cae07). The mean number of alleles per locus was 30. All populations were in Hardy-Weinberg Equilibrium, except for those of Sfax ($P < 0.01$) and Mosrata ($P < 0.001$) (Table 2). The mean observed and expected heterozygosities across loci were 0.855 ± 0.064 and 0.907 ± 0.057, respectively. The mean allelic richness across loci was 12.316 ± 2.952. Weir & Cockerham (1984) estimation of F-Statistics showed that the highest values of F_{IT} (0.155 ± 0.023) and F_{IS} (0.139 ± 0.022) corresponded to locus Cae33, whereas Cae01 exhibited the highest value of F_{ST} (0.023 ± 0.016). Jacknaving and bootstrapping over loci (for 95 and 99 % confidence intervals) showed a higher level of F_{ST} than those recorded for F_{IS} and F_{IT}. The observed and expected heterozygosities and the F_{IS} estimates for the twelve studied populations are shown in Table 2. The mean observed and expected heterozygosities across populations were 0.861 ± 0.038 and 0.907 ± 0.011, respectively. Heterozygosity deficit, as measured by Wright's F_{IS}, showed low levels in most populations when averaged across loci, ranging from -0.008 (population of Monastir) to 0.133 (population of Mosrata) (Table 2). The average value of F_{IS} across populations was 0.050 ± 0.040, indicating a low heterozygote deficiency. This recorded mean F_{IS} value highlighted less important heterozygote deficiency than that considered for the global population (F_{IT} = 0.066 ± 0.029), probably due to the Wahlund effect (Wahlund, 1928).

Table 4. Pairwise comparisons of genetic differentiation estimated from genetic divergence (Φ_{ST}, below the diagonal) and haplotype frequency (F_{ST}, above the diagonal). Values with $P < 0.05$ are reported in bold (significance levels calculated from 10,000 permutations).

| | Western Mediterranean | | | | | Eastern Mediterranean | | | | | | |
	Tabarka	Bizerte	Sidi Rais	Kelibia	Benikhiar	Monastir	Chebba	Sfax	Djerba	Tripoli	Mosrata	Venice
Tabarka	*	0.000	-0.032	-0.045	**0.165**	**0.090**	0.048	**0.088**	**0.098**	0.074	0.056	0.024
Bizerte	0.005	*	0.027	0.028	**0.235**	**0.061**	0.021	**0.055**	**0.061**	**0.067**	0.039	0.024
Sidi Rais	0.005	0.034	*	-0.065	0.131	0.073	0.051	**0.100**	**0.085**	**0.118**	0.035	0.046
Kelibia	0.003	0.029	-0.024	*	0.087	**0.102**	0.069	**0.125**	**0.116**	**0.122**	0.069	0.064
Benikhiar	**0.043**	0.029	**0.032**	**0.044**	*	**0.403**	**0.320**	**0.370**	**0.362**	**0.423**	**0.347**	**0.342**
Monastir	0.066	**0.103**	-0.049	0.043	**0.112**	*	0.012	0.011	0.020	0.024	-0.036	-0.003
Chebba	0.107	**0.141**	-0.014	0.097	0.142	-0.064	*	0.005	0.022	0.015	0.010	0.004
Sfax	**0.517**	**0.553**	**0.400**	**0.516**	**0.560**	**0.264**	**0.191**	*	-0.024	0.029	0.011	0.011
Djerba	**0.259**	**0.300**	0.127	**0.252**	**0.303**	0.021	-0.018	0.042	*	**0.071**	0.009	0.033
Tripoli	0.009	**0.056**	-0.042	0.014	**0.070**	-0.030	-0.010	**0.372**	0.121	*	0.039	0.007
Mosrata	0.114	**0.153**	-0.014	0.095	**0.160**	-0.068	-0.060	**0.213**	-0.018	-0.000	*	-0.011
Venice	0.103	**0.156**	0.044	**0.131**	**0.211**	0.067	0.090	**0.466**	**0.216**	0.011	0.086	*

542

Medit. Mar. Sci., 17/2, 2016, 533-551

Western African Mediterranean
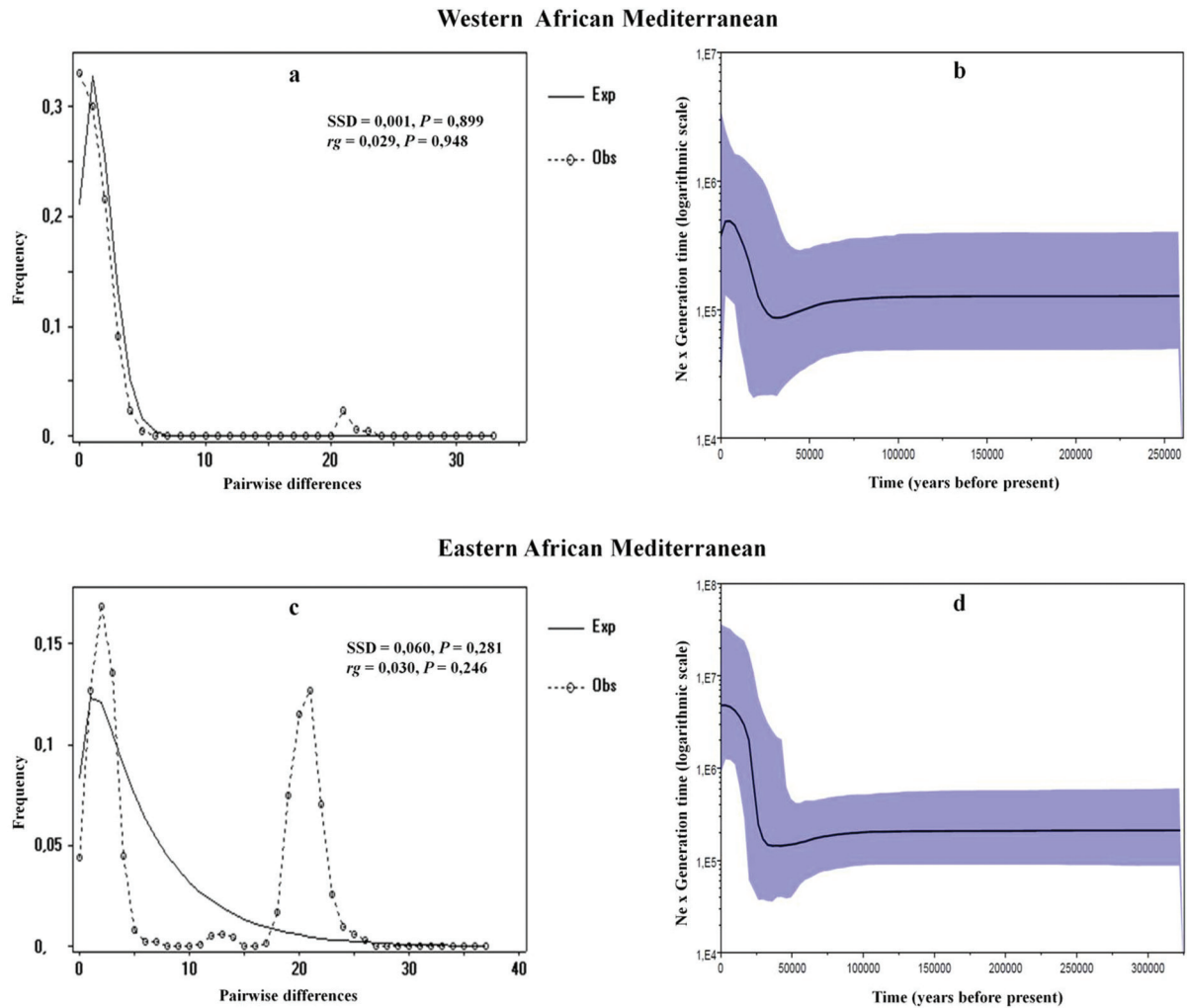
Eastern African Mediterranean

Fig. 4: Mismatch distribution (a, c) and Bayesian skyline plot (BSP, implemented in BEAST) (b, d) for the African Western and Eastern Mediterranean populations of *Carcinus aestuarii*. (a, c) Observed frequencies (dotted line) were compared to the expected frequencies (continuous line), estimated by the growth-decline model implemented in DNASP. The demographic expansion parameters used, τ and $\theta_{initial}$, were calculated in ARLEQUIN; θ_{final} value was fixed at 1000 to simulate the infinite. The two demographic indices SSD and *rg*, provided for the observed mismatch distributions, were calculated under the assumption of a demographic expansion model, implemented in ARLEQUIN. (b, d) BSP plots showing changes in effective population size (Ne multiplied per generation time) over time (measured in years before present). The thick solid line depicts the median estimate, and the margins of the blue area represent the highest 95% posterior density intervals.

Table 5. Neutrality tests (Tajima's D, Fu's F_S, and Ramos-Onsins & Rozas's R_2 tests) and mismatch distribution raggedness index (*rg*) for each population of *Carcinus aestuarii* as well as for the entire sample. Significant values are in bold.

Population	D	F_S	R_2	*rg*
Tabarka	-1.492	-1.507	0.137	0.042
Bizerte	-1.613	**-3.541**	**0.083**	0.064
Sidi Rais	**-1.893**	1.658	0.260	0.094
Kelibia	-1.492	-1.507	**0.137**	0.037
Benikhiar	-1.140	**-0.475**	0.276	0.472
Monastir	-0.660	-1.194	0.122	0.054
Chebba	-0.283	-2.789	0.123	0.051
Sfax	0.735	-2.983	0.160	0.029
Djerba	0.899	1.108	0.168	0.042
Tripoli	-1.481	0.011	0.231	0.158
Mosrata	-0.163	-0.337	0.143	0.077
Venice Lagoon	-0.011	-2.287	0.136	0.080
Whole Data	-0.952	**-24.537**	0.060	0.025

Medit. Mar. Sci., 17/2, 2016, 533-551

543

Overall, our results showed highly significant genetic differentiation among populations. Based on the outcome of the Fisher exact test, we rejected the hypothesis of genetic homogeneity in the distribution of allele frequencies for the entire dataset of microsatellites ($\chi2 = \infty$, ddl = 10, $P < 0.001$). Furthermore, pairwise comparisons of genetic differentiation were significant for most pairs (Table 6). At the genotypic level, the exact test of genetic differentiation (G), implemented in GENEPOP, showed high genotypic differentiation among *C. aestuarii* populations based on the examined loci ($\chi2 = \infty$, ddl = 10, $P < 0.001$). The 1-level AMOVA test also confirmed the hypothesis of a partitioning of genetic variation among populations ($F_{ST} = 0.018$, ddl = 239, $P < 0.001$; Table 3). A significant relationship was found between genetic and geographic distances (r = 0,544, $P = 0,001$) by means of a Mantel Test, supporting an isolation by distance hypothesis to explain population separation. The significant pairwise F_{ST} values are shown in Table 6; they concern mainly comparisons between Western and Eastern Mediterranean populations. Population genetic structure, within the analyzed data, was examined by means of 2-level AMOVA, grouping specimens according to their geographic origin and testing for partitioning of genetic variance under the biogeographic hypothesis

of a separation between the Western Mediterranean and Eastern Mediterranean. Our results showed significant genetic subdivision across the Siculo-Tunisian Strait ($F_{CT} = 0.005$, $P < 0.05$; Table 3). When contrasting the Venice Lagoon population (considered as a particular group of the Adriatic Sea) with those belonging to the Western and Eastern African Mediterranean, the differentiation pattern was more pronounced ($F_{CT} = 0.008$, $P < 0.01$; Table 3). Similarly to the findings with mtDNA, genetic structure, based on microsatellite data and testing only the separation between both African Mediterranean groups (Western vs. Eastern African Mediterranean), was found to be highly significant (2-level AMOVA: $F_{CT} = 0.100$, $P < 0.001$; Table 3).

Population genetic structure was also revealed based on genotypic assignment. The Bayesian inference, implemented in STRUCURE, allowed identifying two divergent genetic clades within the analyzed twelve populations of *C. aestuarii*. The number of possible groups ($K = 2$) corresponded to the highest value of log probability of data (*Ln* P (D) = -3676.6) and was confirmed by the method proposed by Evano *et al.* (2005), showing a clear peak at $K = 2$. The first clade was composed of the populations of Tabarka, Bizerte, Sidi Rais, Kelibia, Benikhiar, Monastir and Chebba, whereas the second clade included those of Sfax, Djerba,
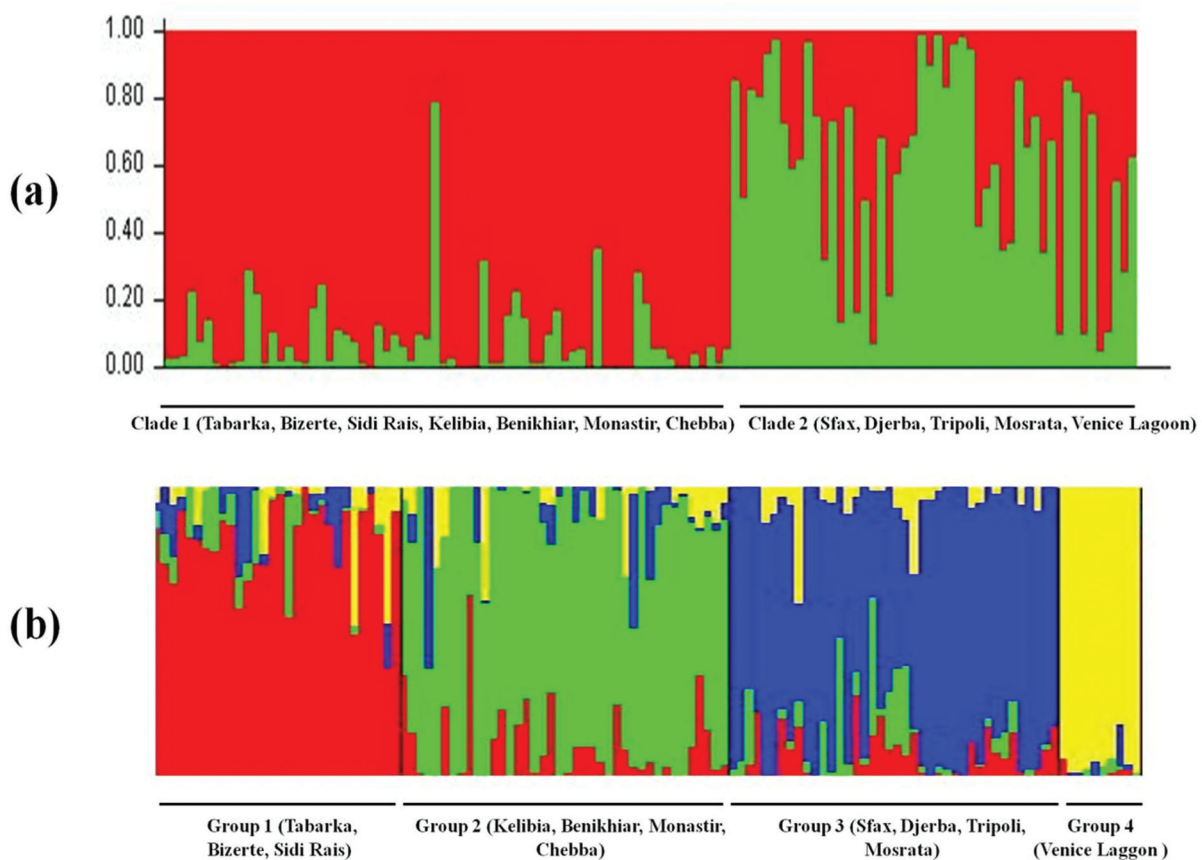

Fig. 5: Population structure of *Carcinus aestuarii* using the Bayesian approach, implemented in STRUCTURE (a) and BAPS (b), to identify clusters of genetically similar populations based on nuclear microsatellite data.

544

Medit. Mar. Sci., 17/2, 2016, 533-551

Table 6. Pairwise comparisons of genetic differentiation estimated from the χ2 of the Fisher exact test (above the diagonal) and the F_{ST} values (below the diagonal). Significant χ2 and F_{ST} differentiation values between populations of *Carcinus aestuarii* are indicated in bold ($P < 0.05$).

	Western Mediterranean					Eastern Mediterranean						
	Tabarka	Bizerte	Sidi Rais	Kelibia	Benikhiar	Monastir	Chebba	Sfax	Djerba	Tripoli	Mosrata	Venice
Tabarka	*	17.690	**24.057**	11.149	15.344	10.284	**21.140**	**42.803**	**26.773**	**34.755**	**18.795**	**47.025**
Bizerte	**0.019**	*	18.267	17.243	13.023	8.654	14.770	**21.660**	**26.669**	**28.361**	15.267	**43.121**
Sidi Rais	0.015	0.012	*	**21.426**	15.915	**26.100**	22.367	**27.182**	**30.215**	**31.534**	**23.863**	**29.254**
Kelibia	0.000	0.000	0.009	*	13.423	9.991	5.433	**26.801**	**25.005**	16.354	**28.520**	**34.889**
Benikhiar	0.008	0.006	0.008	-0.001	*	5.429	9.948	**23.691**	18.050	**26.916**	**24.754**	**28.041**
Monastir	0.006	-0.001	**0.021**	-0.005	-0.010	*	5.056	**20.342**	12.451	**28.198**	18.154	**32.466**
Chebba	**0.033**	0.010	**0.030**	-0.008	0.004	-0.005	*	**23.351**	18.262	**18.806**	15.359	**23.648**
Sfax	**0.038**	0.014	**0.025**	0.014	0.013	0.014	0.017	*	**19.573**	**26.190**	17.800	**27.440**
Djerba	**0.037**	**0.030**	**0.039**	**0.020**	0.011	0.003	0.018	0.019	*	**29.614**	**23.827**	**35.899**
Tripoli	**0.039**	**0.020**	**0.033**	0.005	**0.023**	0.025	0.022	0.025	0.024	*	**23.563**	**27.916**
Mosrata	0.013	0.006	0.016	0.018	0.018	0.015	0.022	0.005	**0.032**	0.026	*	**42.949**
Venice	**0.057**	**0.039**	**0.033**	**0.025**	0.019	**0.026**	0.019	**0.033**	**0.029**	0.021	**0.048**	*

Tripoli, Mosrata and Venice Lagoon (Fig. 5a). Bayesian analysis of population structure inferred from BAPS was more efficient than STRUCTURE in detecting the number of possible genetic groups: BAPS analysis allowed identifying four groups of genetically similar populations ($K = 4$; group 1: Tabarka, Bizerte, Sidi Rais; group 2: Kelibia, Benikhiar, Monastir, Chebba; group 3: Sfax, Djerba, Tripoli, Mosrata; group 4: Venice Lagoon; Fig. 5b), corresponding to the highest log marginal likelihood of the data (log (ml = -3319)) and reflecting a clear subdivision within the two clades obtained by STRUCTURE. AMOVA, based on genotypic grouping, inferred from STRUCTURE and BAPS analyses, also yielded significant allelic structure (AMOVA-based on STRUCTURE grouping: $F_{CT} = 0.006$, $P < 0.01$; AMOVA-based on BAPS grouping: $F_{CT} = 0.010$, $P < 0.001$). It should be pointed out that the results inferred from the BAPS analysis showed an intermediate geographic group (group 2) between the two divergent groups of the Western (group 1) and Eastern African Mediterranean (group 3), which may suggest a possible existence of contact zone across the African Mediterranean coast. The result of genotypic assignment, yielded by the GENECLASS software, showed that 23.30 % of the individuals were correctly attributed (with a quality index of 14.11 %) to the populations from which they were sampled. GENECLASS also revealed that eleven individuals ($P < 0.01$) were potential first generation migrants.

Gene flow analysis within *C. aestuarii* was based on the outcome of genetic structure, focusing mainly on the two African Mediterranean population groups. The statistical approach, implemented in MIGRATE software, recorded an important and asymmetric gene flow between populations of the Western African Mediterranean (group 1: Tabarka, Bizerte, Sidi Rais, Kelibia, Benikhiar) and those of the Eastern African Mediterranean (group 2: Monastir, Chebba, Sfax, Djerba, Tripoli, Mosrata). Gene flow from the first group of populations towards the second group was much more pronounced than the opposite flow (Table 7).

Discussion

The results of this study reveal a non-random distribution of genetic variation in *C. aestuarii* along the central part of the African Mediterranean coast. Based on sequences of the mitochondrial DNA gene COI and nuclear microsatellite data, *F*-statistics and AMOVA

Table 7. Gene flow analysis in African Mediterranean *Carcinus aestuarii*, based on the analysis of microsatellite loci. (Θ: effective size of the population; M: migration rate; group 1: Tabarka, Bizerte, Sidi Rais, Kelibia, Benikhiar; group 2: Monastir, Chebba, Sfax, Djerba, Tripoli, Mosrata).

All loci	Bayesian Analysis : posterior distribution	Acceptance ratios for all parameters and the genealogies	MCMC-Autocorrelation and effective MCMC sample size	
			Autocorrelation	Effective sample size
$\Theta1$	0.097	0.492	0.348	14107.620
$\Theta2$	0.098	0.558	0.489	10573.590
$M2\to1$	14.293	0.382	0.411	10980.190
$M1\to2$	24.471	0.696	0.616	6621.910

Medit. Mar. Sci., 17/2, 2016, 533-551

545

analyses showed a marked genetic structure among African Mediterranean populations of *C. aestuarii*, allowing the identification of two distinct genetic groups and revealing further genetic distinction between both African Mediterranean coastal stretches and the northern Adriatic Sea.

The findings of this investigation are in line with the geographic separation of the Western and Eastern Mediterranean basins, previously described by Marino *et al.* (2011) and Ragionieri & Schubart (2013) for the European Mediterranean populations of *C. aestuarii*, and supports the recent results of Deli *et al.* (2015) that reveal such a differentiation along the Tunisian coast. While these latter investigations and part of our work focus mainly on mtDNA data, our study provides further evidence of nuclear divergence in *C. aestuarii* across the transition zone of the Siculo-Tunisian Strait. Several biotic and abiotic factors potentially leading to genetic differentiation between geographically close populations have been suggested and broadly discussed (Kyle & Boulding, 2000; Selkoe *et al.,* 2008; 2010; Schunter *et al.,* 2011), but their role and respective contributions require further empirical clarifications and support. For instance, we can hypothesize that the genetic differentiation among *C. aestuarii* populations could be the result of regional adaptation to specific abiotic features, such as temperature and salinity. It is known that the Eastern Mediterranean Basin is warmer and more saline than the Western Basin: average water temperatures range between 16 and 29°C, with an average salinity of 39 ppt, as opposed to lower temperatures (12-23°C) and a salinity of 36 ppt in the Western Basin (Serena, 2005).

The genetic distinctiveness of the Lagoon of Venice, noted in our study and in a previous investigation by Ragionieri & Schubart (2013), may also suggest the impact of abiotic features in promoting genetic differentiation, given that the Adriatic Sea has its own characteristics of salinity, temperature, and depth (Maggio *et al.,* 2009). The impact of abiotic features in promoting genetic differentiation has been investigated recently by Jorde *et al.* (2015) who correlated the spatial genetic patterns in the northern shrimp *Pandalus borealis* throughout its North Atlantic distribution zone with geographic distances, patterns of larval drift obtained through oceanographic modelling, and temperature differences, within a multiple linear regression framework. The authors found that bottom temperature differences explained the most multiple genetically distinct groups of the investigated species, indicating a major role played by local adaptation to temperature conditions in promoting evolutionary diversification and speciation in the marine environment. We also think that biotic factors linked to reproduction and recruitment events might have triggered genetic differentiation among the studied green crab populations. Similarly, Marino *et al.* (2010) argued that selective forces acting during recruitment must have given rise to genetic

differentiation among local *C. aestuarii* in the Venitian Lagoon.

Alternatively, historical processes, known to be involved in shaping Mediterranean marine diversity (i.e. the climate fluctuations of the Pleistocene period; see Patarnello *et al.,* 2007), may have triggered such a pattern of divergence in *C. aestuarii*. Phylogenetic relationships between haplotypes, inferred from the statistical parsimony procedure, as well as PERMUT calculations of both levels of population subdivision (N_{ST} and G_{ST}), confirmed the geographic portioning of genetic variation and revealed a significant relationship between phylogeny and the geographical distribution of haplotypes. In this phylogeographical pattern, we distinguished two haplogroups, separated by at least 16 mutational steps, indicating a relatively old separation along the study area and suggesting that both mitochondrial clades had been sendered by long-term biogeographic barriers, and their differentiation was probably maintained by restricted historical gene flow. Our dating procedures, based on the use of different molecular clock models and rates, placed the divergence between the two haplogroups of *C. aestuarii* at 1.91 Myr to 0.69 Myr. This range of divergence time estimation corresponds to the Early Pleistocene (1.8 to about 0.781 Myr; Riccardi, 2009). This period was characterized by strong climate changes and fluctuations in the water level of the Mediterranean Sea (including sporadic isolation from the Atlantic Ocean). These environmental changes may have profoundly affected the genetic structure of the populations of several marine species (see Hewitt, 2000; Patarnello *et al.,* 2007). On the other hand, the contemporary geographic concentration of the second haplogroup (Type II) in Eastern Mediterranean locations (Monastir, Chebba, Sfax, Djerba, Tripoli, Mosrata) might not only reflect the impact of historical events in the region, but rather hint at the influence of a number of abiotic factors such as the thermo-haline circulation system and other physical factors, such as winter surface isotherms that could play an important role in shaping the current species distribution in the Mediterranean Sea (Bianchi & Morri, 2000; Bianchi, 2007).

Demographic history reconstruction, based on the main phylogeographic signal detected in our study, yielded different patterns of demographic history among both African Mediterranean groups. Mismatch distribution analyses recorded a unimodal distribution obtained for the Western African Mediterranean versus a multimodal distribution characterizing the Eastern African group. We could attribute this difference of distribution patterns to the genetic composition of each examined group of populations given that the Western African Mediterranean is characterized mainly by Type I while the Eastern African Mediterranean harbours both differentiated types, I and II, and is thought to be the stronghold of secondary contact between them. Ray *et al.* (2003) stated that multimodal distribution usually characterizes differenti-

546

Medit. Mar. Sci., 17/2, 2016, 533-551

ated populations or populations influenced by migration. Multimodal mismatch distribution may also correspond to demographic growth associated with a subsequent bottleneck (Ray *et al.,* 2003). While both African Mediterranean groups have undergone demographic expansion, as clearly revealed by the combined statistical analyses of mismatch distribution and Bayesian Skyline plots, only the Western group experienced spatial expansion. BSP analyses dated time since expansion for both African Mediterranean regions approximately to the Last Glacial Maximum. During this period, the Mediterranean Sea experienced a dramatic sea-level fluctuation and cold conditions (Waelbroeck *et al.,* 2002; Patarnello *et al.,* 2007). Immediately after the LGM, drastic alterations took place in the Mediterranean Sea, including the rising of the sea level, which might have contributed to the recolonization of different areas in the Mediterranean, i.e. the Adriatic Sea, which flooded 18,000 years ago (Thiede, 1978). Notably, the increase of effective size being much more pronounced in the Eastern group together with the recent time since demographic expansion, suggest recent colonization of the Eastern African Mediterranean, probably originating from refugia present in the Eastern Mediterranean, such as the Sea of Marmara (Peijnenburg *et al.,* 2004). Marino *et al.* (2011) hypothesized that Eastern Mediterranean populations of *C. aestuarii,* probably originated from the adjacent Ionian Sea, could have colonized the Adriatic Sea sometime during the last 18,000 years. In addition, the unimodal distribution and L-shaped BSP trend observed for the Western African Mediterranean strongly suggest a post-glacial spatial expansion event (Crandall *et al.,* 2012). The different effects of Pleistocene glacial cycles on habitat availability may explain the observed differences in demographic tendencies (Kousteni *et al.,* 2014). Hence, the different patterns of demographic history among the different studied African Mediterranean regions suggest that genetic structure could also be affected by population history (Palumbi, 1994; Patarnello *et al.,* 2007).

In general, the particular pattern of genetic divergence among Eastern and Western African Mediterranean populations of *C. aestuarii,* detected by 2-level AMOVA at the mitochondrial level, is consistent with that inferred from microsatellite analyses (AMOVA, STRUCTURE and BAPS). This phylogeographical pattern, verified by both mitochondrial and nuclear markers, is interestingly in congruence with previous morphometric investigations of green crab populations from the same region, which showed strong morphometric differentiation between Eastern and Western Mediterranean populations (Deli *et al.,* 2014). The concordance of genetic and phenotypic characters in defining two distinct groups of *C. aestuarii* suggests geographic separation, triggered by divergent selection pressures between alternative environments, and may hint at a possible signature of historical events that took place in the study region and might have

shaped the genetic structure of many marine species, such as fishes (Bahri-Sfar *et al.,* 2000; Mejri *et al.,* 2009; Kaouèche *et al.,* 2011), molluscs (Gharbi *et al.,* 2011), and shrimps (Zitari-Chatti *et al.,* 2008; 2009). The striking similarity of biogeographic patterns reinforces the idea that these Mediterranean species were probably facing the same historical events and strongly suggests vicariance events during Pleistocene glacial episodes characterized by strong climate fluctuations (Thiede, 1978).

Indeed, the Pleistocene was characterized by a succession of abrupt climate changes, involving alternating glacial and interglacial periods (Lisiecki & Raymo, 2007). In the Mediterranean Sea, temperature and sea level fluctuations led to the fragmentation of the distribution range of marine species on either side of the Siculo-Tunisian Strait (Thiede, 1978; Pielou, 1979; Nilsson, 1983; Peres, 1985). It should be noted that during the last glacial maximum, the Eastern Basin was warmer than the Western Basin, with a temperature difference of about 10°C between the basins according to Thiede (1978), and this temperature gradient is preserved until present (Mojetta & Ghisotti, 1996). It is therefore quite possible that the ancient separation between the populations of the two Mediterranean basins allowed the accumulation of significant variations over time, thus offering the opportunity to diverge during the last two million years. This divergence is currently maintained by a restricted contemporary gene flow across the Siculo-Tunisian Strait, as revealed by the nuclear microsatellite analysis. In this context, the pattern of nuclear differentiation could be attributed to the pattern of sea surface currents across the study region. Contemporary water circulation along the North African littoral is characterized by a unidirectional surface current called 'the Algerian current' originating from the Atlantic, which moves eastwards along the North African coast and only leaves the coastal zone opposite the north coast of Tunisia (around Kelibia), close to the border of the Eastern Mediterranean Basin (see main surface currents in Fig. 1). There is no local surface current in the opposite direction, and the Eastern Mediterranean Basin is characterized by very weak circulation (Pinardi & Masetti, 2000). Therefore, larvae (as the main dispersal stage) drifting in the surface water layers would move along the northern Tunisian coast and homogenize populations there, but could not reach the south-eastern populations. Water currents would probably transport *C. aestuarii* larvae away from the eastern Tunisian and Libyan populations to locations farther northeast in the Mediterranean and may lead to reduced connectivity along the African coastline.

Despite the significant genetic structure of the Mediterranean green crab *C. aestuarii,* recorded between the two basins of the Mediterranean, the distribution pattern of the two haplogroups along the African Mediterranean coast showed haplotype mixing in the Eastern Mediterranean (types I and II). As already invoked by Ragionieri

Medit. Mar. Sci., 17/2, 2016, 533-551

547

& Schubart (2013), such results indicate that the Western Mediterranean Basin might have played a crucial role as a source of genetic variability for the Eastern Basin, at least during the recent past. Therefore, the remarkable co-existence of the two types in Eastern African Mediterranean populations highlights the possibility of secondary contact between already differentiated genetic groups. This result seems to be consolidated by the nuclear data, inferred from the Bayesian analysis of genetic structure (BAPS), showing an intermediate geographic group (group 2) between the two divergent groups of the Western (group 1) and Eastern African Mediterranean (group 3). Although this hypothetical contact area, thought to be located at the Siculo-Tunisian Strait, still needs to be verified, the asymmetric gene flow (from the Western to the Eastern African Mediterranean), as inferred by the results of the MIGRATE analysis, reinforces the previously mentioned results and supports the hypothesis of a secondary contact between two historically isolated groups. In addition, the reported asymmetric gene flow (in a west-east direction) confirms this phenomenon in *C. aestuarii*, as already highlighted based on mtDNA analysis by Ragionieri & Schubart (2013). This is in agreement with the main circulation systems of the study region.

In summary, the overall results allow us to advance the following hypothesis: During periods of Early Pleistocene glaciations, regressing sea levels limited the biotic exchange across the Siculo-Tunisian Strait. The Eastern Basin was more influenced by these environmental changes and experienced more or less important desiccation episodes in different parts (Meijer & Krijgsman, 2005). Thus, being separated from the rest of the Mediterranean, an endemic fauna of the Eastern Mediterranean may have originated and evolved a particular and different genetic composition. In this context, haplogroup Type II may correspond to an eastern Mediterranean endemic isolate, originating from climate oscillations during the Pleistocene. Several biological and geological pieces of evidence support the existence of refuge zones or isolates in the Eastern Mediterranean (Pielou, 1979; Peres, 1985). Subsequently, the secondary contact between populations of the two basins might have been promoted through recolonization episodes, mediated mainly by the rise in sea level. In a study focused on the genetic structure of *Posidonia oceanica* in the Mediterranean, Arnaud-Haond *et al.* (2007) showed the existence of significant nuclear divergence between the two basins of the Mediterranean, with the remarkable existence of a relatively high allelic richness in the Siculo-Tunisian Strait region (considered a secondary contact zone). These authors also hypothesized a vicariant phenomenon in this species followed by secondary contact.

Finally, the haplotypic composition found so far in *C. aestuarii* along different parts of its distribution range (European and African Mediterranean) suggests a complex evolutionary history of the species and invokes the existence of a vicariant event across the Siculo-Tunisian Strait, as shown by mitochondrial and nuclear markers. These insights are very important and suggest that the green crab consists of several genetic stocks in the Mediterranean Sea. Further genetic investigations, stretching to more distant locations in the Eastern Mediterranean, are required to characterize and delineate these evolutionary units in more detail.

References

Almaca, C., 1962. Sur la distribution géographique du genre *Carcinus* Leach (Crust. Dec. Brach.). *Revista da Faculdade de Ciências da Universidade de Lisboa*, 10, 109-113.

Arnaud-Haond, S., Diaz Almela, E., Teixeira, S., 2007. Vicariance patterns in the Mediterranean Sea: East-West cleavage and low dispersal in the endemic seagrass *Posidonia oceanica*. *Journal of Biogeography*, 14, 963-976.

Astraldi, M., Balopoulos, S., Candela, J., Font, J., Gacic, M. *et al.,* 1999. The role of straits and channels in understanding the characteristics of Mediterranean circulation. *Progress in Oceanography*, 44, 65-108.

Bahri-Sfar, L., Lemaire, C., Ben Hassine, O.K., Bonhomme, F., 2000. Fragmentation of sea bass populations in the western and eastern Mediterranean as revealed by microsatellite polymorphism. *Proceedings of the Royal Society of London B*, 267, 929-935.

Beerli, P., 2006. Comparison of Bayesian and maximum-likelihood inference of population genetic parameters. *Bioinformatics*, 22 (3), 341-345.

Beerli, P., Felsenstein, J., 2001. Maximum likelihood estimation of migration rates and effective population numbers in two populations using a coalescent approach. *Proceedings of the National Academy of Sciences of the United States*, 98, 4563-4568.

Behrens Yamada, S., Hauck, L., 2001. Field identification of the European green crab species: *Carcinus maenas* and *Carcinus aestuarii*. *Journal of Shellfish Research*, 20, 905-912.

Béranger, K., Mortier, L., Gasparini, G.P., Gervasio, L., Astraldi, M. *et al.,* 2004. The dynamics of the Sicily Strait: a comprehensive study from observations and models. *Deep-Sea Research II*, 51, 411-440.

Bianchi, C.N., 2007. Biodiversity issues for the forthcoming tropical Mediterranean Sea. *Hydrobiologia*, 580, 7-21.

548

Medit. Mar. Sci., 17/2, 2016, 533-551

Bianchi, C.N., Morri, C., 2000. Marine biodiversity of the Mediterranean Sea: situation, problems and prospects for future research. *Marine Pollution Bulletin*, 40, 367-376.

Borsa, P., Blanquer, A., Berrebi, P., 1997. Genetic structure of the flounders *Platichthys flesus* and *P. stellatus* at different geographic scales. *Marine Biology*, 129, 233-246.

Brookfield, J.F.Y., 1996. A simple new method for estimating null allele frequency from heterozygote deficiency. *Molecular Ecology*, 5, 453-455.

Bulnheim, H.P., Bahns, S., 1996. Genetic variation and divergence in the genus *Carcinus* (Crustacea, Decapoda). *Internationale Revue der Gesamten Hydrobiologie*, 81, 611-619.

Burridge, C.P, Craw, D., Fletcher, D., Waters, J.M., 2008. Geological dates and molecular rates: Fish DNA sheds light on time dependency. *Molecular Biology and Evolution*, 25, 624-633.

Carlton, J.T., Cohen, A.N., 2003. Episodic global dispersal in shallow water marine organisms: the case history of the European shore crabs *Carcinus maenas* and *C. aestuarii*. *Journal of Biogeography*, 30, 1809-1820.

Clark, P.F., Neale, M., Rainbow, P.S., 2001. A morphometric analysis of regional variation in *Carcinus* Leach, 1814 (Brachyura: Portunidae: Carcininae) with particular reference to the status of the two species *C. maenas* (Linnaeus, 1758) and *C. aestuarii* (Nardo, 1847). *Journal of Crustacean Biology*, 21 (1), 288-303.

Clark, P.U., Dyke, A.S., Shakun, J.D., Carlson, A.E., Clark, J. *et al.,* 2009. The last glacial maximum. *Science*, 325, 710-714.

Clement, M., Posada, D., Crandall, K., 2000. TCS: A computer program to estimate gene genealogies. *Molecular Ecology*, 9, 1657-1660.

Collina-Girard, J., 2001. L'Atlantide devant le détroit de Gibraltar ? Mythe et géologie. *Comptes Rendus de l'Académie des Sciences, Paris (2a)*, 333 (4), 233-240.

Corander, J., Waldmann, P., Sillanpaa, M.J., 2003. Bayesian analysis of genetic differentiation between populations. *Genetics*, 163, 367-374.

Crandall, E.D., Sbrocco, E.J., Deboer, T.S., Barber, P.H., Carpenter, K.E., 2012. Expansion dating: calibrating molecular clocks in marine species from expansions onto the Sunda Shelf following the Last Glacial Maximum. *Molecular Biology and Evolution*, 29, 707-719.

Darling, J.A., Bagley, J.M., Roman, J., Tepolt, C.K., Geller, J.B., 2008. Genetic patterns across multiple introductions of the globally invasive crab genus *Carcinus*. *Molecular Ecology*, 17, 4992-5007.

Deli, T., Said, K., Chatti, N., 2014. Morphological differentiation among geographically close populations of the green crab *Carcinus aestuarii* Nardo, 1847 (Brachyura, Carcinidae) from the Tunisian coast. *Crustaceana*, 87 (3), 257-283.

Deli, T., Said, K., Chatti, N., 2015. Genetic differentiation among populations of the green crab *Carcinus aestuarii* (Brachyura, Carcinidae) from the Eastern and Western Mediterranean coasts of Tunisia. *Acta Zoologica Bulgarica*, 67 (3), 327-335.

Demeusy, N., 1958. Recherches sur la mue de puberté du décapode brachyoure *Carcinus maenas* Linné. *Archives de Zoologie Expérimentale et Générale*, 95, 253-492.

Drummond, A.J., Ho, S.Y.W., Phillips, M.J., Rambaut, A., 2006. Relaxed phylogenetics and dating with confidence. *PLoS Biology*, 4, e88.

Drummond, A.J., Rambaut, A., Shapiro, B., Pybus, O.G., 2005. Bayesian coalescent inference of past population dynamics from molecular sequences. *Molecular Biology and Evolution*, 22, 1185-1192.

Drummond, A.J., Suchard, M.A., Xie, D., Rambaut, A., 2012. Bayesian phylogenetics with BEAUti and the BEAST 1.7. *Molecular Biology and Evolution*, 29, 1969-1973.

Dupanloup, I., Schneider, S., Excoffier, L., 2002. A simulated approach to define the genetic structure of populations. *Molecular Ecology*, 11, 2571-2581.

Evanno, G., Regnaut, S., Goudet, J., 2005. Detecting the number of clusters of individuals using the software STRUCTURE: A simulation study. *Molecular Ecology*, 14, 2611-2620.

Excoffier, L., 2004. Patterns of DNA sequence diversity and genetic structure after a range expansion: Lessons from the infinite-island model. *Molecular Ecology*, 13, 853-864.

Excoffier, L., Laval, G., Schneider, S., 2005. Arlequin ver. 3.0: An integrated software package for population genetics data analysis. *Evolutionary Bioinformatics Online*, 1, 47-50.

Excoffier, L., Smouse, P.E., Quattro, J.M., 1992. Analysis of molecular variance inferred from metric distances among DNA haplotypes: application to human mitochondrial DNA restriction data. *Genetics*, 131, 479-491.

François, O., Durand, E., 2010. Spatially explicit Bayesian clustering models in population genetics. *Molecular Ecology Resources*, doi: 10.1111/j.1755-0998.2010.02868.x.

Furota, T., Watanabe, S., Watanabe, T., Akiyama, S., Kinoshita, K., 1999. Life history of the Mediterranean green crab, *Carcinus aestuarii* Nardo, in Tokyo Bay, Japan. *Crustacean Research*, 28, 5-15.

Fu, Y.X., 1997. Statistical tests of neutrality of mutations against population growth, hitchhiking and background selection. *Genetics,* 147, 915-925.

Geller, J.B., Walton, E., Grosholz, E., Ruiz, G.M., 1997. Cryptic invasions of the crab *Carcinus* detected by molecular phylogeny. *Molecular Ecology*, 6, 256-262.

Gharbi, A., Zitari-Chatti, R., Van Womhoudt, A., Dhraief, M.N., Denis, F. *et al.,* 2011. Allozyme variation and population genetic structure in the carpet shell clam *Ruditapes decussatus* across the Siculo-Tunisian Strait. *Biochemical Genetics*, 49, 788-805.

Goudet, J., 1995. FSTAT (version 1.2): A computer program to calculate F-statistics. *Journal of Heredity*, 86, 485-486.

Grant, W.S., 2015. Problems and cautions with sequence mismatch analysis and Bayesian Skyline Plots to infer historical demography. *Journal of Heredity*, 106 (4), 333-346.

Hall, T.A., 1999. BioEdit: A user-friendly biological sequence alignment editor and analysis program for Windows 95 / 98 / NT. *Nucleic Acids Symposium Series*, 41, 95-98.

Harpending, H.C., 1994. Signature of ancient population growth in a low-resolution mitochondrial DNA mismatch distribution. *Human Biology*, 66 (4), 591-600.

Hewitt, G.M., 2000. The genetic legacy of the Quaternary ice ages. *Nature*, 405, 907-913.

Hilbish, T.J., 1996. Population genetics of marine species: the interaction of natural selection and historically differentiated populations. *Journal of Experimental Marine Biology and Ecology*, 200, 67-83.

Hsü, K.J., Montadert, L., Bernoulli, D., Cita, M.B., Erickson, A. *et al.,* 1977. History of the Mediterranean salinity crisis. *Nature*, 267, 399-403.

Hudson, R.R., 1990. Gene genealogies and the coalescent process. p. 1–44. In: *Oxford surveys in evolutionary biology*. Fu-

tuyama, D., Antonovics, J.D. (EDs). Oxford University Press, Oxford.

Jorde, P.E., Vik, G.S., Westgaard, J-I., Albretsen, J., André, C. *et al.,* 2015. Genetically distinct populations of northern shrimp, *Pandalus borealis*, in the North Atlantic: adaptation to different temperatures as an isolation factor. *Molecular Ecology*, 24, 1742-1757.

Kaouèche, M., Bahri-Sfar, L., González-Wangüemert, M., Pérez-Ruzaf, Á., Ben Hassine, O.K., 2011. Allozyme and mtDNA variation of white seabream *Diplodus sargus* populations in a transition area between western and eastern Mediterranean basins (Siculo-Tunisian Strait). *African Journal of Marine Science*, 33 (1), 79-90.

Knowlton, N., Weigt, L.A., 1998. New dates and new rates for divergence across the Isthmus of Panama. *Proceeding of Royal Society of London*, 265, 2257-2263.

Kousteni, V., Kasapidis, P., Kotoulas, G., Megalofonou, P., 2014. Strong population genetic structure and contrasting demographic histories for the small-spotted catshark (*Scyliorhinus canicula*) in the Mediterranean Sea. *Heredity*, doi:10.1038/hdy.2014.107.

Krijgsman, W., Hilgen, F.J., Raffi, I., Sierro, F.J., Wilson, D.S., 1999. Chronology, causes and progression of the Messinian salinity crisis. *Nature*, 400, 652-655.

Kyle, C.J., Boulding, E.G., 2000. Comparative population genetic structure of marine gastropods (*Littorina spp.*) with and without pelagic larval dispersal. *Marine Biology*, 137, 835-845.

Latch, E.K., Dharmarajan, G., Glaubitz, J.C., Rhodes, O.E., 2006. Relative performance of Bayesian clustering software for inferring population substructure and individual assignment at low levels of population differentiation. *Conservation Genetics*, 7, 295-302.

Librado, P., Rozas, J., 2009. DnaSP v5: A software for comprehensive analysis of DNA polymorphism data. *Bioinformatics*, 25, 1451-1452.

Lisiecki, L.E., Raymo, M.E., 2007. Plio-Pleistocene climate evolution: trends and transitions in glacial cycle dynamics. *Quaternary Science Reviews*, 26, 56-69.

Maggio, T., Lo Brutto, S., Garoia, F., Tinti, F., Arculeo, M., 2009. Microsatellite analysis of red mullet *Mullus barbatus* (Perciformes, Mullidae) reveals the isolation of the Adriatic Basin in the Mediterranean Sea. *ICES Journal of Marine Science*, 66, 1-9.

Marino, I.A.M., Barbisan, F., Gennari, M., Bisol, P.M., Zane, L., 2008. Isolation and characterization of microsatellite loci in the Mediterranean shore crab *Carcinus aestuarii* (Decapoda, Portunidae). *Molecular Ecology Resources*, 8, 370-372.

Marino, I.A.M., Barbisan, F., Gennari, M., Giomi, F., Beltramini, M. *et al.,* 2010. Genetic heterogeneity in populations of the Mediterranean shore crab, *Carcinus aestuarii* (Decapoda, Portunidae), from the Venice Lagoon. *Estuarine, Coastal and Shelf Science*, 87, 135-144.

Marino, I.A.M., Pujolar, J.M., Zane, L., 2011. Reconciling deep calibration and demographic history: Bayesian Inference of post glacial colonization patterns in *Carcinus aestuarii* (Nardo, 1847) and *C. maenas* (Linnaeus, 1758). *PLoS ONE*, 6 (12), e28567.

Meijer, P.T., Krijgsman, W., 2005. A quantitative analysis of the dessication and re-filling of the Mediterranean during the Messinian Salinity Crisis. *Earth and Planetary Science Letters*, 240, 510-520.

Mejri, R., Lo Brutto, S., Ben Hassine, O.K., Arculeo, M., 2009. A study on *Pomatoschistus tortonesei* Miller 1968 (Perciformes, Gobiidae) reveals the Siculo-Tunisian Strait (STS) as a breakpoint to gene flow in the Mediterranean basin. *Molecular Phylogenetics and Evolution*, 53, 596-601.

Miller, M.P., 2005. Alleles In Space: Computer software for the joint analysis of Interindividual spatial and genetic information. *Journal of Heredity*, 96, 722-724.

Mistri, M., Rossi, R., Fano, E.A., 2001. Structure and secondary production of a soft bottom macrobenthic community in a brackish lagoon (Sacca di Goro, northeastern Italy). *Estuarine, Coastal and Shelf Science*, 52, 605-616.

Mojetta, A., Ghisotti, A., 1996. *Flore et faune de la Méditerranée*. Solar publication, Paris, 318 pp.

Mori, M., Mancon, R., Fanciulli, G., 1990. Notes on the reproductive biology of *Carcinus aestuarii* Nardo (Crustacea, Decapoda) from the lagoon of San Teodoro (Island of Sardinia, Italy). *Rivista di Idrobiologia*, 29, 763-774.

Nei, M., 1987. *Molecular Euolutionary Genetics*. Columbia University Press, New York, 512 pp.

Nikula, R., Vainola, R., 2003. Phylogeography of *Cerastoderma glaucum* (Bivalvia: Cardiidae) across Europe: a major break in the Eastern Mediterranean. *Marine Biology*, 143, 339-350.

Nilsson, T., 1983. *The Pleistocene*. Enke, Stuttgart, 651 pp.

Paetkau, D., Calvert, W., Stirling, I., Strobeck, C., 1995. Microsatellite analysis of population structure in Canadian polar bears. *Molecular Ecology*, 4, 347-354.

Paetkau, D., Slade, R., Burden, M., Estoup, A., 2004. Genetic assignment methods for the direct, real-time estimation of migration rate: A simulation-based exploration of accuracy and power. *Molecular Ecology*, 13, 55-65.

Palumbi, S.R., 1994. Genetic divergence, reproductive isolation, and marine speciation. *Annual Review of Ecology and Systematics*, 25, 547-572.

Palumbi, S.R., Grabowski, G., Duda, T., Geyer, L., Tachino, N., 1997. Speciation and population genetic structure in tropical Pacific sea urchins. *Evolution*, 51, 1506-1517.

Patarnello, T., Volckaert, F.A.M., Castilho, R., 2007. Pillars of Hercules: Is the Atlantic-Mediterranean transition a phylogeographical break? *Molecular Ecology*, 16, 4426-4444.

Peijnenburg, K.T.C., Breeuwer, J.A.J., Pierrot-Bults, A.C., Menken, S.B.J., 2004. Phylogeography of the planktonic chaetognath *Sagitta setosa* reveals isolation in European seas. *Evolution*, 58, 1472-1487.

Peres, J.M., 1985. History of the Mediterranean biota and the colonization of the depths. p. 198-232. In: *Western Mediterranean – Key Environment Series*. Margalef, R. (EDs). Pergamon, Oxford.

Petit, R.J., Hampe, A., Cheddadi, R., 2005. Climate changes and tree phylogeography in the Mediterranean. *Taxon*, 54, 877-885.

Pielou, E.C., 1979. *Biogeography*. Wiley, New York, 351 pp.

Pinardi, N., Masetti, E., 2000. Variability of the large scale general circulation of the Mediterranean Sea from observations and modelling: A review. *Paleogeography, Paleoclimatology, Paleoecology*, 158, 153-174.

Piry, S., Alapetite, A., Cornuet, J.M., Paetkau, D., Baudouin, L. *et al.,* 2004. GENECLASS2: A software for genetic assignment and first-generation migrant detection. *Journal of Heredity*, 95, 536-539.

550

Medit. Mar. Sci., 17/2, 2016, 533-551

Pons, O., Petit, R.J., 1995. Estimation, variance and optimal sampling of gene diversity. *Theoretical and Applied Genetics*, 90, 462-470.

Pons, O., Petit, R.J., 1996. Measuring and testing genetic differentiation with ordered versus unordered alleles. *Genetics*, 144, 1237-1245.

Posada, D., Crandall, K.A., 1998. Modeltest: testing the model of DNA substitution. *Bioinformatics*, 14, 817-818.

Pritchard, J.K., Stephens, M., Donnelly, P., 2000. Inference of population structure using multilocus genotype data. *Genetics*, 155, 945-959.

Quesada, H., Beynon, C.M., Skibinski, D.O.F., 1995. A mitochondrial DNA discontinuity in the mussel *Mytilus Galloprovincialis* Lmk: Pleistocene vicariance biogeography and secondary intergradations. *Molecular Biology and Evolution*, 12, 521-524.

Ragionieri, L., Schubart, C.D., 2013. Population genetics, gene flow, and biogeographical boundaries of *Carcinus aestuarii* (Crustacea: Brachyura: Carcinidae) along the European Mediterranean coast. *Biological Journal of the Linnean Society*, 109, 771-790.

Rambaut, A., 2009. FigTree v1.3.1. Computer program available at: http: // tree.bio.ed.ac.uk / software / figtree/

Rambaut, A., Drummond, A.J., 2007. Tracer v 1.4.8. Institute of Evolutionary Biology, University of Edinburg, Available from: http//beast.edu.ac.uk/Tracer

Ramos-Onsins, S.E., Rozas, J., 2002. Statistical properties of new neutrality tests against population growth. *Molecular Biology and Evolution*, 19, 2092-2100.

Rannala, B., Mountain, J.L., 1997. Detecting immigration by using multilocus genotypes. *Proceedings of the National Academy of Sciences of the United States*, 94, 9197-9201.

Rannala, B., Yang, Z., 1996. Probability distribution of molecular evolutionary trees: A new method of phylogenetic inference. *Journal of Molecular Evolution*, 43, 304-311.

Ray, N., Currat, M., Excoffier, L., 2003. Intra-deme molecular diversity in spatially expanding populations. *Molecular Biology and Evolution*, 20, 76-86.

Raymond, M., Rousset, F., 1995. GENEPOP (version 1.2): Population genetics software for exact tests and ecumenicism. *Journal of Heredity*, 86, 248-249.

Riccardi, A.C., 2009. IUGS ratified ICS Recommendation on redefinition of Pleistocene and formal definition of base Quaternary. International Union of Geological Sciences.

Roman, J., Palumbi, S.R., 2004. A global invader at home: population structure of the green crab *Carcinus maenas* in Europe. *Molecular Ecology*, 13, 2891-2898.

Schubart, C.D., 2009. Mitochondrial DNA and decapod phylogenies: The importance of pseudogenes and primer optimization. p. 47–65. In: *Crustacean Issues 18 – Decapod Crustacean Phylogenetics*. Martin, J.W., Crandall, K.A., Felder, D.L. (EDs). Taylor and Francis/CRC Press Boca Raton, Florida.

Schunter, C., Carreras-Carbonell, J., Macpherson, E., Tintore, J., Vidal-Vijande, E. *et al.,* 2011. Matching genetics with oceanography: Directional gene flow in a Mediterranean fish species. *Molecular Ecology*, 20, 5167-5181.

Selkoe, K.A., Henzler, C.M., Gaines, S.D., 2008. Seascape genetics and the spatial ecology of marine populations. *Fish and Fisheries*, 9, 363-377.

Selkoe, K.A., Watson, J.R., White, C., Ben Horin, T., Iacchei, M. *et al.,* 2010. Taking the chaos out of genetic patchiness: seascape genetics reveals ecological and oceanographic drivers of genetic patterns in three temperate reef species. *Molecular Ecology*, 19, 3708-3726.

Serena, F., 2005. Field identification guide to the sharks and rays of the Mediterranean and Black Sea. p. 97. In: *FAO Species identification Guide for Fishery Purposes*. FAO, Rome.

Simon, C., Frati, F., Beckenbach, A., Crespi, B., Liu, H. *et al.,* 1994. Evolution, weighting, and phylogenetic utility of mitochondrial gene sequences and a compilation of conserved polymerase chain reaction primers. *Annals of the Entomological Society of America*, 87, 651-701.

Tajima, F., 1983. Evolutionary relationships of DNA sequences in finite populations. *Genetics*, 105, 437-460.

Tajima, F., Nei, M., 1984. Estimation of evolutionary distance between nucleotide sequences. *Molecular Biology and Evolution*, 1, 269-285.

Tajima, F., 1989. The effect of change in population size on DNA polymorphism. *Genetics Society of America*, 123, 597-601.

Tamura, K., Peterson, D., Peterson, N., Stecher, G., Nei, M. *et al.,* 2011. MEGA5: Molecular evolutionary genetics analysis using maximum likelihood, evolutionary distance, and maximum parsimony methods. *Molecular Biology and Evolution*, 28, 2731-2739.

Templeton, A.R., Crandall, K.A., Sing, C.F., 1992. A cladistic analysis of phenotypic associations with haplotypes inferred from restriction endonuclease mapping and DNA sequence data. III. Cladogram estimation. *Genetics*, 132, 619-633.

Thiede, J., 1978. A glacial Mediterranean. *Nature*, 276, 680-683.

van Oosterhout, C., Hutchinson, W.F., Wills, D.P.M., Shipley, P., 2004. MICRO-CHECKER: Software for identifying and correcting genotyping errors in microsatellite data. *Molecular Ecology Notes*, 4, 535-538.

Waelbroeck, C., Labeyrie, L., Michel, E., Duplessy, J.C., McManus, J.F. *et al.,* 2002. Sea-level and deep water temperature changes derived from benthic foraminifera isotopic records. *Quaternary Science Reviews*, 21, 295-305.

Waples, R.S., 1998. Separating the wheat from the chaff: patterns of genetic differentiation in high gene flow species. *Journal of Heredity*, 89, 438-450.

Weir, B.S., Cockerham, C.C., 1984. Estimating F-Statistics for the Analysis of Population Structure. *Evolution*, 38 (6), 1358-1370.

Wahlund, S., 1928. Zusammersetung von Populationen und Korrelation-sercheinungen von Standpunkt der Verebungslehre aus betrachtet. *Hereditas*, 11, 65-106.

Yang, Z., Rannala, B., 1997. Bayesian phylogenetic inference using DNA sequences: a Markov chain Monte Carlo method. *Molecular Biology and Evolution*, 14, 717-724.

Zitari-Chatti, R., Chatti, N., Elouaer, A., Said, K., 2008. Genetic variation and population structure of the caramote prawn *Penaeus kerathurus* (Forskal) from the eastern and western Mediterranean coasts in Tunisia. *Aquaculture Research*, 39, 70-76.

Zitari-Chatti, R., Chatti, N., Fulgione, D., Gaiazza, I., Aprea, G. *et al.,* 2009. Mitochondrial DNA variation in the caramote prawn *Penaeus* (*Melicertus*) *kerathurus* across a transition zone in the Mediterranean Sea. *Genetica*, 136, 439-447.

Medit. Mar. Sci., 17/2, 2016, 533-551

551